Sónia Raquel Nunes Henriques

Microglia as cellular targets for immunomodulation during neurodevelopment

Master's Thesis in Biomedical Research

2015

· U C ·

Universidade de Coimbra

Cover image: manually drawn microglial cell, representative of the morphology in the adult brain parenchyma.

Microglia as cellular targets for immunomodulation during neurodevelopment

Sónia Raquel Nunes Henriques

Dissertation presented to the Faculty of Medicine of the University of Coimbra for the meeting of the necessary requirements to the obtainment of the Master degree in Biomedical Research. The work was performed in the Retinal Dysfunction and Neuroinflammation Lab of the Institute for Biomedical Imaging and Life Sciences (IBILI), Faculty of Medicine, University of Coimbra under the scientific supervision of Doctor Catarina A. Reis Vale Gomes and co-supervision of Doctor António Francisco Rosa Gomes Ambrósio.

University of Coimbra

2015

The experimental tasks described in the present thesis were developed at the Institute for Biomedical Imaging and Life Sciences (IBILI), University of Coimbra, Portugal. Samples were obtained with the indispensable support of the Life and Health Sciences Research Institute (ICVS), University of Minho, Portugal.

Financial support was granted by the Research Support Office (GAI, Faculty of Medicine, University of Coimbra, Portugal), the Foundation for Science and Technology, Portugal (Strategic Projects: Pest C/SAU/UI3282/2013 and Pest UID/NEU/04539/2013), COMPETE-FEDER, and Santander Totta.

Acknowledgments

Em primeiro lugar, um imenso obrigada aos meus maravilhosos pais, Manuela e José Maria Henriques. Nenhum pequeno parágrafo conseguirá alguma vez exprimir a imensa gratidão que sinto pelo apoio e carinho incondicionais. Este trabalho é muito vosso também.

Ao Marcelo Henriques, por todo o interesse pelo meu trabalho e prontidão para me aconselhar – um verdadeiro irmão mais velho.

Um vasto agradecimento à Doutora Catarina Gomes, não só por me permitir embarcar num projeto tão envolvente, mas também por me proporcionar uma perspetiva muito mais aliciante do que é fazer ciência. Um sincero obrigada por todos os ensinamentos e todos os conselhos que sempre levarei comigo.

Ao Doutor Francisco Ambrósio, por me ter aceite no seu laboratório e, sobretudo, me ter proporcionado todas as condições para um trabalho frutífero.

Ao Doutor Henrique Girão, por me ter dado a oportunidade de ingressar num mestrado que me permitiu crescer imenso, tal como esperava que acontecesse.

Fundamental foi também o Doutor Rodrigo Cunha, que sempre que lhe foi possível assegurou a continuidade deste projeto. Da mesma forma, agradeço à equipa do Doutor Nuno Sousa, no Instituto de Ciências da Vida e Saúde (ICVS), Universidade do Minho, pela disponibilidade e auxílio ao longo do projeto.

Indispensáveis à conclusão deste mestrado foram também a Filipa Gomes e a Rita Gouveia. Não existe problema que não diminua de dimensão com uma gargalhada genuína e uma boa dose de relativização.

À Filipa Batista devo também grande parte desta tese. Não me cruzei com ninguém mais prestável e gentil, mais disposta a ajudar o outro. Obrigada por tudo o que me ensinaste e pela paciência que tiveste – ambos em quantidades generosas.

Ao João Martins, um agradecimento pela criação do melhor ambiente de trabalho que poderia alguma vez desejar.

A todos os colegas de laboratório que sempre estiveram dispostos a ajudar e a ensinar; a repreender e a corrigir; a fazer melhores cientistas uma pipetagem de cada vez.

Table of Contents

Figures and Table Index

Figures

Tables

Abbreviations List

$A_{2A}R$	Adenosine A_{2A} receptors
ADP	Adenosine diphosphate
AMP	Adenosine monophosphate
ANOVA	Analysis of variance
ATP	Adenosine triphosphate
BCA	Bicinchoninic acid
BDNF	Brain-derived neurotrophic factor
BSA	Bovine serum albumin
cAMP	Cyclic adenosine monophosphate
CNS	Central nervous system
CORT	Corticosterone
COX-2	Cyclo-oxygenase-2
CUS	Chronic unpredictable stress
CXCL10	Chemokine (C-X-C motif) ligand 10
DAPI	4',6-diamidino-2-phenylindole
DEX	Dexamethasone
DNA	Deoxyribonucleic acid
DTT	Dithiothreitol
ECF	Enhanced chemofluorescent
ECL	Enhanced chemoluminescent
ED	Embryonic day
GC	Glucocorticoids
GR	Glucocorticod receptors
G_s	Stimulatory G proteins
HPA	Hypothalamic-pituitary-adrenal
Iba-1	Ionized calcium-binding adapter molecule 1
IL-1β	Interleukin-1β
IL-6	Interleukin-6
ip	Intraperitoneally

***iu*DEX**	*In utero* DEX
LPS	Lipopolyssaccharide
MR	Mineralocorticod receptors
NAcc	*Nucleus accumbens*
NGF	Nerve growth factor
NO	Nitric oxide
PBS	Phosphate buffered saline
PFC	Prefrontal cortex
PGE2	Prostaglandin E2
PND	Post-natal day
ROS	Reactive oxygen species
RPMI	Roswell Park Memorial Institute
RT	Room temperature
Sal	Saline
sc	Subcutaneously
SDS	Sodium dodecyl sulfate
SEM	Standard error of the mean
TBS-T	Tris-buffered saline with tween 20
TEMED	N,N,N',N'-tetramethylethylenediamine
TNF-α	Tumor necrosis factor- α

Abstract

Dexamethasone (DEX) is a synthetic glucocorticoid often used in the clinical practice to prevent the respiratory complications associated with preterm deliveries. However, subjects treated with this immunosupressor tend to be pathologically anxious and liable to depression. Studies with animal models mimicking this therapy have reported that *in utero* DEX (*iu*DEX) has deleterious effects on the central nervous system (CNS), such as neuronal apoptosis, synaptic loss and dendritic atrophy. The mechanism responsible for these effects remains unclear. Microglia emerge as potential candidates for mediating the aforementioned alterations because, besides having functional glucocorticoid receptors (GR), they are fundamental cells during neurodevelopment, participating in the formation and elimination of synapses. Moreover, it has been shown that *iu*DEX alters microglia morphology at post-natal day (PND) 1, 7 and 90. Microglial dynamics is controlled by adenosine A_{2A} receptors ($A_{2A}R$), also involved in the pathophysiology of anxiety and depression and in the alterations of dendritic branching present in stressed individuals.

First, a study was conducted *in vitro* to assess if DEX (1 μM) could have a direct impact on microglial cells (N9 cell line) morphology and to evaluate the ability of $A_{2A}R$ blockade to modulate DEX effects (using the selective antagonist SCH58261, 50 nM). *In vivo* experiments were performed using female Wistar rats exposed to *iu*DEX on embryonic day (ED) 18 and 19 (1 mg/kg/day subcutaneously [sc] to pregnant rats) and chronically treated with SCH58261 (0.1 mg/kg/day intraperitoneally [ip]) or saline, with several objectives: (1) to evaluate the physiological role of $A_{2A}R$ in the control of microglial morphology; and (2) to evaluate the ability of $A_{2A}R$ blockade to revert DEX-mediated effects on microglial morphology in the prefrontal cortex (PFC), a core brain region in mood disorders. In parallel, it was considered of relevance (3) to evaluate the impact of *iu*DEX on the density of $A_{2A}R$ and GR, screened throughout different brain regions; and (4) to perform correlation analyses between the corticosterone (CORT, the physiological glucocorticoid in rodents) levels in the serum and (a) the behavioural phenotype – anxiety and depression (unpublished data) – and (b) the reproductive cycle (termed estrous cycle, in rodents).

In preliminary *in vitro* studies, DEX tended to alter the ramified to amoeboid cells ratio, which was reversed by pre-incubation with the $A_{2A}R$ antagonist.
Animals exposed to *iu*DEX exhibited differences in the density of GR and $A_{2A}R$, which were dependent on the brain region analysed.

The morphometric analysis revealed that *iu*DEX affected microglial morphology, globally decreasing both the number and length of branches. $A_{2A}R$ blockade *per se* diminished the number and length of processes, an effect exacerbated in animals previously exposed to *iu*DEX.
Animals subjected to *iu*DEX presented altered levels of serum CORT, which was also observed in animals chronically treated with the $A_{2A}R$ antagonist at adulthood.
Additionally, the results indicate that the behaviour of the female rats was not correlated with estrous cycle or CORT levels.

Altogether, these results indicate that the adenosinergic system is altered by *iu*DEX. Data also demonstrate that microglia is not only affected by *iu*DEX in the early stages of life, but that these alterations persist in adulthood. Moreover, microglia morphology is also considerably altered by the blockade of $A_{2A}R$ in adulthood, revealing a quite important role for these receptors in a physiological situation.

Key words: Microglia, Neurodevelopment, Dexamethasone, Adenosine A_{2A} Receptors.

Resumo

A dexametasona (DEX) é um glucocorticóide sintético frequentemente usado na prática clínica para prevenir as complicações respiratórias associadas a partos prematuros. Contudo, indivíduos tratados com este imunossupressor têm tendência a ser patologicamente ansiosos e suscetíveis à depressão. Estudos com modelos animais mimetizando esta terapia mostram que a DEX *in utero* (*iu*DEX) tem efeitos prejudiciais no sistema nervoso central (CNS), tais como apoptose neuronal, perda sinática e atrofia dendrítica. O mecanismo responsável por estes efeitos ainda não se encontra esclarecido. A microglia surge como um potencial candidato para mediar os efeitos mencionados porque, além de possuir recetores de glucocorticóides (GR), é uma célula fundamental durante o neurodesenvolvimento, participando na formação e eliminação de sinapses. Além disso, já foi demonstrado que a *iu*DEX altera a morfologia da microglia no dia pós-natal (PND) 1, 7 e 90. A dinâmica microglial é controlada pelos recetores de adenosina A_{2A} (A_{2A}R), também envolvidos na fisiopatologia da ansiedade e depressão e nas alterações da ramificação dendrítica presentes em indivíduos com stress.

Em primeiro lugar, um estudo foi conduzido *in vitro* para avaliar se a DEX (1 μM) poderia ter um efeito direto na morfologia de células da microglia (linha celular N9) e para avaliar se o bloqueio dos A_{2A}R modularia os efeitos da DEX (utilizando o antagonista seletivo SCH58261, 50 nM). Experiências *in vivo* foram realizadas com fêmeas de ratos Wistar expostas a *iu*DEX no dia embrionário (ED) 18 e19 (1 mg/kg/dia subcutaneamente [sc] a fêmeas de rato grávidas) e cronicamente tratadas com SCH58261 (0.1 mg/kg/dia intraperitonealmente [ip]) ou salino, com vários objetivos: (1) avaliar o papel fisiológico dos A_{2A}R no controlo da morfologia da microglia; e (2) avaliar se o bloqueio dos A_{2A}R é eficaz na reversão dos efeitos mediados pela DEX na morfologia da microglia no córtex prefrontal (PFC), uma região do cérebro com um papel central em distúrbios de humor. Paralelamente, foi considerado relevante (3) avaliar o impacto da *iu*DEX na densidade de A_{2A}R e GR, avaliada em várias regiões do cérebro; e (4) efetuar análises de correlação entre os níveis de corticosterona (CORT, o glucocorticóide fisiológico em roedores) no plasma e (a) o fenótipo comportamental – ansiedade e depressão (dados não publicados) – e (b) o ciclo reprodutivo (denominado ciclo éstrico em roedores).

Em estudos preliminares *in vitro*, a DEX tendeu a alterar o rácio entre células ramificadas e amebóides, o que foi prevenido pela pré-incubação com o antagonista dos A_{2A}R.

Animais expostos a *iu*DEX exibiram diferenças na densidade de GR e $A_{2A}R$, dependendo da região do cérebro analisada.

A análise morfométrica revelou que a *iu*DEX afeta a morfologia da microglia, diminuindo globalmente tanto o número como o comprimento das ramificações. O bloqueio dos $A_{2A}R$ *per se* diminuiu o número e comprimento dos processos, um efeito exacerbado em animais previamente expostos a *iu*DEX.

Animais sujeitos a *iu*DEX apresentaram níveis alterados de CORT no plasma, o que também foi observado em animais cronicamente tratados com SCH58261 na idade adulta.

Adicionalmente, os resultados indicam que o comportamento de fêmeas de rato não esteve correlacionado com o ciclo éstrico ou com os níveis de CORT.

Em conjunto, estes resultados indicam que o sistema adenosinérgico é alterado pela *iu*DEX. Os dados demonstram também que a microglia não é apenas afetada pela iuDEX em fases iniciais da vida, mas que estas alterações permanecem na idade adulta. Além disso, a morfologia da microglia está também alterada na idade adulta pelo bloqueio dos $A_{2A}R$, revelando um papel bastante importante destes recetores numa situação fisiológica.

Palavras-chave: Microglia, Neurodesenvolvimento, Dexametasona, Recetores de adenosina A_{2A}.

CHAPTER 1

INTRODUCTION

1.1. Microglial roles in the healthy brain

1.1.1. Brain colonization and differentiation

Microglia are macrophage-like cells that inhabit, exclusively, the central nervous system (CNS). Part of the innate immunity of the brain (Kettenmann et al., 2011), macrophages originated from the progenitor mesodermal cells will, once inside the CNS, differentiate into mature microglial cells (Ginhoux et al., 2010, Ginhoux et al., 2013). Progenitor mesodermal cells give rise to primitive macrophage progenitors in the yolk sac; these will differentiate into microglia after colonizing the brain early in development at embryonic day (ED) 9.5 (Ginhoux et al., 2010), a process illustrated in fig. 1. Microglial proliferation peaks between PND (post-natal day) 6 and 9; however, this does not translate into an increase in density until PND 9 due to the increase in brain size during early stages of development (Dalmau et al., 2003).

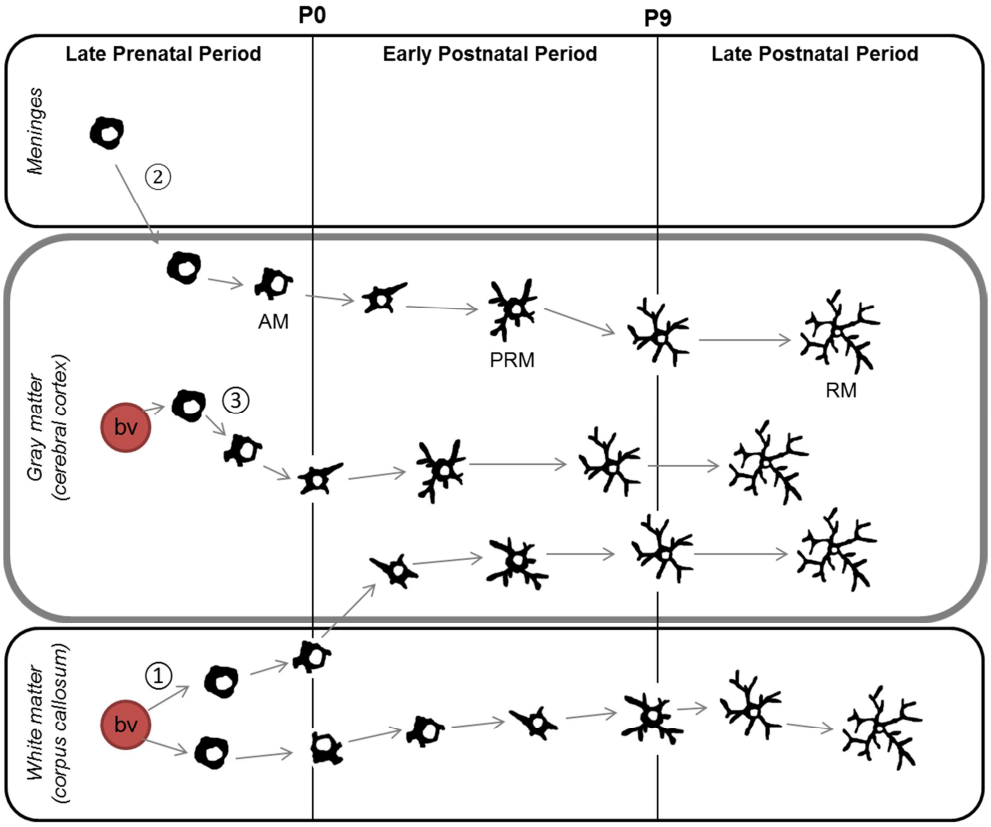

Figure 1. Schematic representation of microglial colonization of the brain during neurodevelopment. Microglia may enter the brain through different routes, including the vascular system of the white (1) and grey (3) matter and meninges encompassing grey matter (2). Apoptosis is also a relevant factor in this developmental route, allowing the speculation about transitory populations of microglial cells with particular purposes. AM, amoeboid microglia; PRM, primitive ramified microglia; RM, resting microglia; bv, blood vessels (based on Dalmau et al., 2003).

Microglial cells during neurodevelopment are much less ramified than those found in an adult individual. Only after PND 0 these cells begin to acquire a more ramified shape, fully extending their processes approximately two weeks after birth in rats (Dalmau et al., 1998). Recently, a subpopulation of cells in the yolk sac was identified as selectively expressing the *slc7a7* gene, marking these cells for microglia differentiation and presenting itself as necessary for colonization of the brain. This discovery allows identifying, before arriving at the host-tissue, cells predetermined to a particular differentiation path (Rossi et al., 2015).

1.1.2. Microglial physiology: from the classical point of view to the shifted paradigms

For a long time, microglia was thought to be well characterized, in particular the correlation between morphology and function (Tremblay et al., 2015). A ramified profile was associated with a "resting state", where microglia would be inactive. In a pathological context, this cell would transit to an "activated state", becoming amoeboid. At this stage, microglia would become phagocytic in order to eliminate cell debris, apoptotic cells or invading pathogens (Graeber, 2010). Secretion of pro- or anti-inflammatory cytokines would occur in parallel with this transformation (Frank et al., 2007, Michaud et al., 2015).

The idea that prevailed for many years that microglia was only responsible for managing the inflammatory response when brain homeostasis became threatened has lost strength in the field over the last decade (Kettenmann et al., 2013). The first evidence of microglial activity in physiological conditions occurred when movement of processes was detected in fluorescently labelled microglia through two-photon tracking, in the undisturbed brain environment (Davalos et al., 2005; Nimmerjahn et al., 2005), proving that this cell is dynamic even in the absence of an insult. This discovery stimulated the research in the field, as it is shown in fig. 2. Under the control of adenosine triphosphate (ATP), an indicator of neuronal activity, this movement is not random throughout the brain (Davalos et al., 2005), but a survey system that approaches synapses (approximately once per hour) according to neuronal activity: if it is reduced, so is the frequency of microglial synaptic contacts (Wake et al., 2009). For instance, sensory experiences, namely light deprivation, are capable of modulating microglial movements (Tremblay et al., 2010). This synaptic juxtaposition of microglia can be located at pre- and post-synaptic sites, synaptic clefts, axon terminals and perisynaptic astrocytic processes (Tremblay et al., 2010), as illustrated in fig. 3.

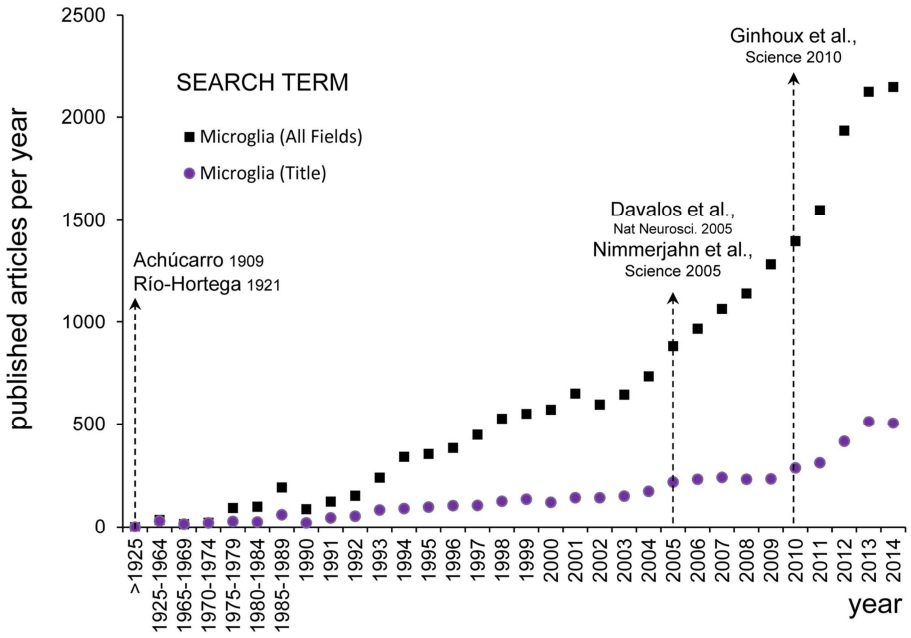

Figure 2. The growth of research involving microglia. Since the first discoveries of this cell, its growing importance has been indisputable (PubMed Data: www.ncbi.nlm.nih.gov). Despite the constant increase of the interest of the scientific community in these cells, the article by Davalos describing the physiological activity of microglia, as well as Ginhoux's evidences of microglial origins (the yolk sac) have instigated the field and stimulated further research, here assessed by the number of articles containing the term "microglia" in the title or in any field (Tremblay et al., 2015).

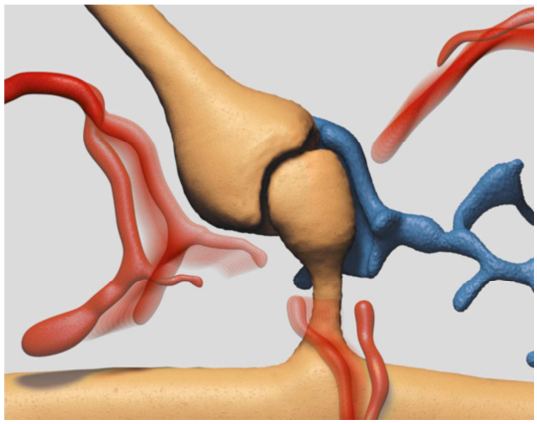

Figure 3. Microglial juxtaposition to other brain cells. Highly dynamic microglial cells (in red) may contact not only with neurons (in beige), pre- and post-synaptically, but also with astrocytes (in blue) (Kettenmann et al., 2013).

Microglia are the professional phagocytes of the brain, excelling at that (Magnus et al., 2002). However, a misconception that stood for many years was that microglia needed to be amoeboid to phagocyte debris (Sierra et al., 2013). That dogma was also deconstructed with reports of ramified microglia phagocyting cellular debris in a physiological context (Sierra et al., 2010).

During neurodevelopment, microglia also play an important role in shaping the brain circuitry. Besides secreting trophic factors, such as nerve growth factor (NGF; Frade et al., 1998) and neurotrophin-3 (NT-3; Elkabes et al., 1998), these cells also control the number of neural precursor cells through phagocytosis (Cunningham et al., 2013). Synaptic pruning, a process by which extranumerary synapses are eliminated in the developing brain, is recognized as critical for a long time (Rakic et al., 1986). Still, only in the past years it became clear that microglia was a key element for this process in neurodevelopment, phagocyting synaptic elements in the post-natal period (Paolicelli et al., 2011). However, microglial cells also contribute to the formation of new synapses (Cristóvão et al., 2014) in a brain-derived neurotrophic factor (BDNF)- and interleukin-10 (IL-10)-dependent manner (Lim et al., 2013; Parkhurst et al., 2013). All these observations have made it indisputable that microglia is absolutely fundamental for the maturation of the brain, conditioning neuronal survival and balancing the number of functional synapses.

1.2. Dexamethasone: a major clinical tool with pervasive effects in brain development

1.2.1. Glucocorticoid hormones

Corticosteroids are a family of hormones involved in several physiological processes, some of which are stress coping and immune response (Vandevyver et al., 2013). Two main classes can be distinguished: mineralocorticoids and glucocorticoids (GC), with receptors associated with each category. Different hormones of each class are not exclusive to that receptor (Reul et al., 1987).

In humans, the most abundant GC is cortisol, meeting its equivalent in corticosterone (CORT), in rodents. Both have affinity towards mineralocorticoid receptors (MR) and glucocorticoid receptors (GR), even though a 10-fold greater affinity to MR results in a basal activation of these (Reul et al., 1987; Sapolsky et al., 1999). Because MR and GR are associated with neuroprotective and neurodegenerative processes, respectively, lower or higher levels of CORT disrupt this balance and negatively impact, for example, on hippocampal-dependent learning and synaptic excitability (Sousa et al., 1999; Sousa et al., 2000; Sousa et al., 2002, Sapolsky et al., 1999). The aforementioned deleterious outcomes associated with increases or decreases of basal CORT levels originate a graphical representation of the effects of cortisol coincident with an “inversed U” pattern (Sorrells et al., 2009).

In the plasma, approximately 90 % of total corticosteroids bind to a circulating protein termed corticosteroid-binding globulin (CBG). The remaining 10 %, free or bound to albumin, will act on target cells and trigger specific responses. Dexamethasone (DEX), however, being a synthetic agonist for GR, has much less affinity to CBG (Cooke et al., 1996) and, consequently, circulates bound to albumin, significantly increasing its power of action relatively to, for instance, cortisol. DEX can also cross the blood brain barrier, gaining facilitated access to the CNS (Meijer et al., 1998) and the placenta during pregnancy (Smith et al., 1988).

1.2.2. The hypothalamic-pituitary-adrenal axis physiology

GC are both synthesised and secreted in the adrenal cortex in a circadian rhythm (24 h system): their production is greater during the activity period (day for humans and night for rodents), peaking at the beginning of this interval (Chung et al., 2011). The synthesis of these hormones is regulated by a system called hypothalamic-pituitary-adrenal (HPA) axis, finely tuned through the negative feedback exerted by circulating hormones (Sapolsky et al., 1986; Waffarn et al., 2012). Internal and external signals trigger the hypothalamus to produce corticotropin-releasing hormone (CRH), which will stimulate the anterior pituitary to produce and release adrenocorticotropic hormone (ACTH). The latter will, finally, exert its action on the adrenal cortex, the responsible for secreting GC. As in various classical feedback mechanisms, GC will act upon the hypothalamus and the pituitary to stop the flow of the respective hormones (fig. 4).

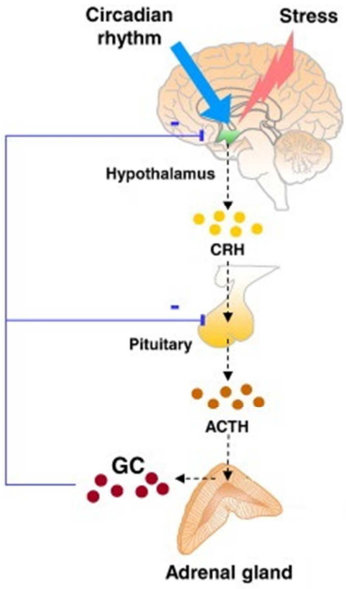

Figure 4. Regulation of the hypothalamic-pituitary-adrenal axis. When circadian or stress signals activate the axis, the hypothalamus releases CRH that will, in turn, stimulate the secretion of ACTH by the pituitary. This will culminate in the production and the release of GC by the adrenal gland, responsible for exerting negative feedback on the other

components of the axis, as well as acting on other targets. HPA, hypothalamic-pituitary-adrenal; CRH, corticotropin-releasing hormone; ACTH, adrenocorticotropic hormone; GC, glucocorticoids (adapted from Chung et al., 2011).

During a stress situation, the stressor agent will activate the HPA axis and, therefore, increase the levels of circulating GC (Sapolsky et al., 1986; Waffarn et al., 2012). These stressor agents may be physical, namely low levels of glucose, or emotional, such as the sight of danger, an information that needs to be processed cortically before passing on to the hypothalamus (Sawchenko et al., 1996; Herman et al., 1997).

The HPA axis is regulated by more than one brain region, the major ones being the prefrontal cortex (PFC), the hippocampus and the amygdala (Herman et al., 2005) which exhibit a high density of GR (de Kloet et al., 1998; Sanchéz et al., 2000). In fact, it has been stated that over-activation of GR leads to a decreased volume in the PFC (essential for mood control) (Banasr et al., 2008; Cerqueira et al., 2005) and hippocampus (involved in learning and memory) (Sousa et al., 1999). In the latter region, over-exposure to CORT also debilitates neurogenesis (Silva et al., 2008) and cognition and decreases spine density (Sousa et al., 2000). The PFC and the hippocampus are not fully independent when it comes to control the HPA axis, once chronic stress interferes with the coherence of the communication between cortico-limbic structures (ventral hippocampus and medial PFC) (Oliveira et al., 2013).

1.2.3. Dexamethasone signalling through glucocorticoid receptors

DEX binds selectively to GR. This receptor, expressed in neurons and glial cells, is distributed ubiquitously in the brain, particularly concentrated in a few regions such as the hippocampus and the PFC (de Kloet et al., 1998). In the hippocampus, GR expression is unchanged by age; in the PFC it increases in adolescents and adults, comparing with infants and aged individuals (Perlman et al., 2007). As an element of the nuclear receptor superfamily of ligand-dependent transcription factors, this receptor can be found in the cytoplasm forming a complex that includes more than one chaperone (Lu et al., 2006). However, when the ligand crosses the membrane (DEX is highly lipophilic) and binds to GR, the chaperone proteins are released and the receptor may exert its actions through three different routes: (1) directly binding to deoxyribonucleic acid (DNA), (2) coupling with other proteins that will directly interact with DNA or (3) regulating the activity of several kinases located in the cytoplasm, as illustrated in fig. 5 (Oakley et al., 2013).

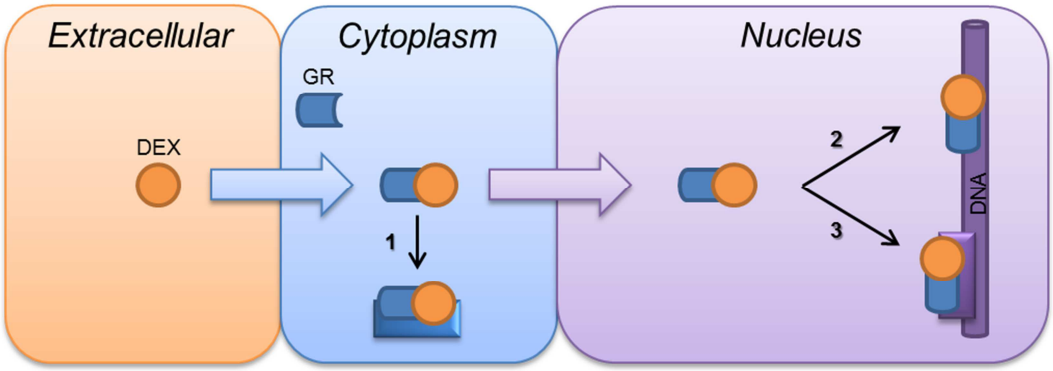

Figure 5. Dexamethasone signalling cascade through binding to glucocorticoid receptors. Circulating DEX is highly lipophilic and, therefore, crosses the cell membrane passively. Once inside the cell, it binds to GR (cytoplasmic receptors). DEX, now bound to GR, can exert its effects in three different ways: (1) altering the activity of diverse kinases or, after translocating into the nucleus, (2) directly interacting with DNA or (3) interacting with DNA-bound transcription factors, up- or down-regulating gene expression.

1.2.4. Clinical importance of glucocorticoids

GC are a resource in the clinics mainly due to their anti-inflammatory and immunosupressive properties (Brownfoot et al., 2013; Drozdowicz et al., 2014). For these particular effects, the active GR directly bind to DNA, up-regulating anti-inflammatory genes and, on the other hand, down-regulating pro-inflammatory genes (Rizzo et al., 2007).

The described mechanism renders GC extremely useful in a myriad of medical conditions, mainly inflammatory and immune diseases, from allergies and skin diseases to congenital adrenal hyperplasia and some leukaemias. The administration may be acute or chronic and the therapeutic protocols are variable, as well. The pronounced positive outcomes are paralleled by side effects: osteoporosis, *diabetes mellitus*, redistribution of body fat, euphoria, depression and, occasionally, psychosis (Lewis et al., 1983; Drozdowicz et al., 2014).

1.2.4.1. Dexamethasone as a prenatal therapy

A particular circumstance justifying the use of DEX is preterm childbirth. When delivery occurs prematurely, the incidence of lung inflammation is quite common due to infections and mechanical ventilation, generating a condition named bronchopulmonary dysplasia, which very often used to lead to a very high morbidity associated with prematurity. The introduction of DEX administration briefly before childbirth significantly decreased the levels of morbidity through the amelioration or even prevention of this inflammation (Brownfoot et al., 2013; Drozdowicz et al., 2014).

Prenatal administration of DEX to rodents has been associated, during the past few years, to deleterious effects, not only related to brain wiring (Dias Heijtz et al., 2010; Leão et al., 2007), but also, in terms of behaviour, with animals presenting anxiety-like behaviour and being significantly more prone to depression (lack of ability to cope with stressful situations) in adulthood (Oliveira et al., 2006; Nagano et al., 2008; Oliveira et al., 2012). In several regimens of administration, DEX has been proven to induce neuronal loss and dendritic impairment in the PFC (Cerqueira et al., 2005; Cerqueira et al., 2007), as well as neuronal damage or apoptosis in the striatum and hippocampus (Sousa et al., 1998; Haynes et al., 2001). Also in the hippocampus, it has been demonstrated that over-stimulation of GR leads to dendritic atrophy and synaptic loss (Sousa et al., 2000).

Because the alterations previously mentioned could be relevant when taking place in critical time points of neurodevelopment, studies have also been conducted with models mimicking the protocols of administration of DEX in humans. Those same studies have reported that prenatal DEX is responsible for persistent alterations that include genetic reprogramming (reduced GR mRNA levels) in the PFC (Diaz Heijtz et al. 2010) and diminished volume and number of cells in the *nucleus accumbens* (NAcc; Leão et al., 2007). In addition, variations (higher and lower) in the number of dopaminergic neurons in both the ventral tegmental area (VTA) and the *substantia nigra pars compacta* (SNc) upon prenatal administration of DEX have been reported (McArthur et al., 2005; Leão et al., 2007). Additionally, it has been shown that prenatal DEX increases the number of immature synapses (Rodrigues et al., 2011).

Prenatal DEX extends its effects to the developing HPA axis. Animals exposed to DEX *in utero* (*iu*DEX) manifest altered levels of corticosteroids, an effect dependent on the gender and drug regimen (Levitt et al., 1996; Liu et al., 2001). Illustrating that, in Wistar rats, DEX administration for five days close to the end of gestation originated elevated basal levels of corticosteroids in males (Levitt et al., 1996). However, in guinea pigs, intermittent injection of the same glucocorticoid during pregnancy originates lower levels of cortisol in males. In females, the opposite happens, an effect reversed depending on the luteal phase of the reproductive cycle (Liu et al., 2001).

1.2.5. Involvement of microglia in the interaction between neuroinflammation and glucocorticoid-mediated responses

Unlike what would be expected, GC response is not always anti-inflammatory in the CNS: acute stress leads to an increase in the levels of cyclo-oxygenase-2 (COX-2) [enzyme that produces prostaglandin E2 (PGE2), a generator of immune response

(Ricciotti et al., 2012)] in the cortex (Madrigal et al., 2003). It has also been shown that animals with higher levels of basal CORT are more prone to the accumulation of pro-inflammatory factors (Perez-Nievas et al., 2007). The correlation between stress and inflammatory responses is not clearly defined, as it may be influenced by a number of variables, a subject reviewed by Sorrells et al., 2009. One of them is the exposure time point: in one study, when GC (hormones that become increased during a stress event) are administered before the inflammatory trigger lipopolysaccharide (LPS, a bacterial endotoxin), the levels of hippocampal IL-1β and tumor necrosis factor- α (TNF-α), pro-inflammatory cytokines, increase. However, the effect is the opposite when LPS precedes GC (Frank et al., 2010). Secondly, analyses carried out between different brain regions are also different. In a scenario of chronic unpredictable stress (CUS) followed by inflammation, nuclear factor kappa β (NF-kβ) binding activity is enhanced in the hippocampus and frontal cortex, but not in the hypothalamus (Munhoz et al., 2006). Even though the reasons for these differences are not completely clarified, it should be taken in consideration the relative distribution of GR and MR across the brain, once it is not homogenous (de Kloet et al., 2000).

Microglia, being a macrophage-like cell that expresses GR (Sierra et al., 2008), is involved in the inflammatory response of the CNS to increased levels of GC. Even though there is a lack of information regarding this particular interaction from a morphological point of view, the way microglia in particular influences the inflammatory *milieu* has been approached. *In vitro*, RAW 264.7 cells (macrophages cell line) enhanced the LPS-induced release of TNF-α, interleukin-6 (IL-6) and nitric oxide (NO) when CORT was administered 24-12h (but not 6-0h) before the immune challenge (Smyth et al., 2004). Accordingly, 30 min of pre-incubation with DEX diminishes reactive oxygen species (ROS) production in the BV-2 microglial cell line (Huo et al., 2011).

Translating to a more realistic model, microglia isolated from animals pre-treated with CORT respond to LPS with upregulation of major histocompatibility complex II (MHCII) and toll-like receptor-4 (TLR-4) and overexpression of IL-1β, IL-6 and TNF-α (Frank et al., 2010). Moreover, subacute stress increases microglial proliferation in a GR-dependent manner (Nair et al., 2006). Therefore, the literature suggests that GC are able to prevent neuroinflammation (Sugama et al., 2013).

1.3. Adenosine receptors in the brain

1.3.1. Adenosine physiological roles and metabolism

Adenosine is a signalling molecule of the purines group. It has numerous functions in the CNS, from the modulation of synaptic transmission to the control of synaptic plasticity (Dias et al., 2013). There, adenosine has a double function: it acts as a neuromodulator (controlling neurotransmitters release) and as a homeostatic messenger (Cunha et al., 2001; Gomes et al., 2011). Variations in adenosine levels are also related with the energy balance of the tissue: as an illustration, in a hypoxic scenario, characterized by a much greater energy demand, the levels of adenosine rise dramatically as a result of ATP hydrolysis (Newby et al., 1991).

Adenosine can be produced intra- or extracellularly (fig. 6). Intracellularly, it may originate from adenosine monophosphate (AMP; degraded by an intracellular 5'-nucleotidase) (Zimmerman et al., 1998) or from the hydrolysis of S-adenosyl-homocysteine (Broch et al., 1980). Extracellularly, the sources are AMP, adenosine diphosphate (ADP) or ATP, all of them broken down into adenosine, directly or sequentially, by ectonucleotidases. Another possible extracellular origin is cyclic adenosine monophosphate (cAMP), metabolized into adenosine through a phosphodiesterase, even though this particular source is not physiologically relevant (Brundege et al., 1997). If adenosine levels rise excessively, it is transported into the cells and phosphorylated by adenosine kinase into AMP or degraded into inosine by adenosine deaminase. The latter enzyme is also present extracellularly (Lloyd et al., 1995).

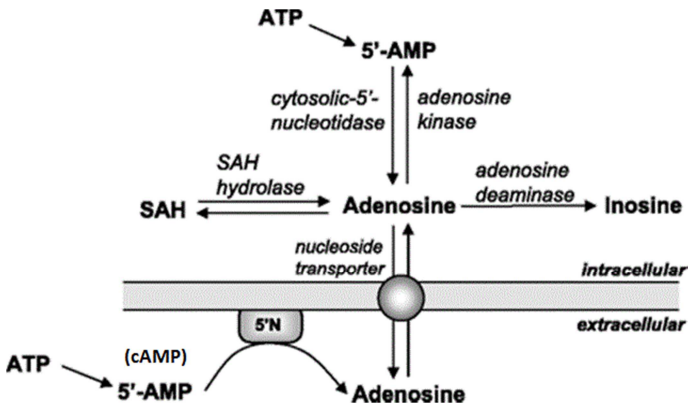

Figure 6. Adenosine production and degradation. Adenosine can be produced in- and outside the cell. Intracellularly, it may originate from AMP or from SAH or be degraded into inosine. Extracellularly, adenosine may also be formed by

dephosphorilation of AMP or from cAMP (not relevant in balancing adenosine levels). AMP, adenosine monophosphate; ATP, adenosine monophosphate; cAMP, cyclic adenosine monophosphate; SAH, S-adenosyl-homocysteine; 5′N, ecto-5′-nucleotidase (adapted from Adair, 2005).

In terms of transport, adenosine usually crosses the cell membrane by facilitated diffusion through equilibrative nucleoside transport proteins (ENT 1 and 2) to balance the intra- and extracellular levels of adenosine. When, in some tissues, this balance is not desirable, adenosine may be transported against the gradient through concentrative nucleoside transport proteins (CNT 1 and 2) (Baldwin et al., 1999; Latini et al., 2001).

1.3.2. Adenosine receptors

There are four different adenosine receptors cloned so far: A_1, A_{2A}, A_{2B} and A_3. (Fredholm et al., 2001). They are not solely activated by adenosine (e.g. inosine [Jin et al., 1997]), but it is the principal agonist for the four of them. Adenosine is also not exclusive to these receptors (the human growth hormone secretagogue receptor is a target as well [Tullin et al., 2000]); still, the great part of its action is mediated by adenosine receptors to be found in several body organs (Fredholm et al., 2005).

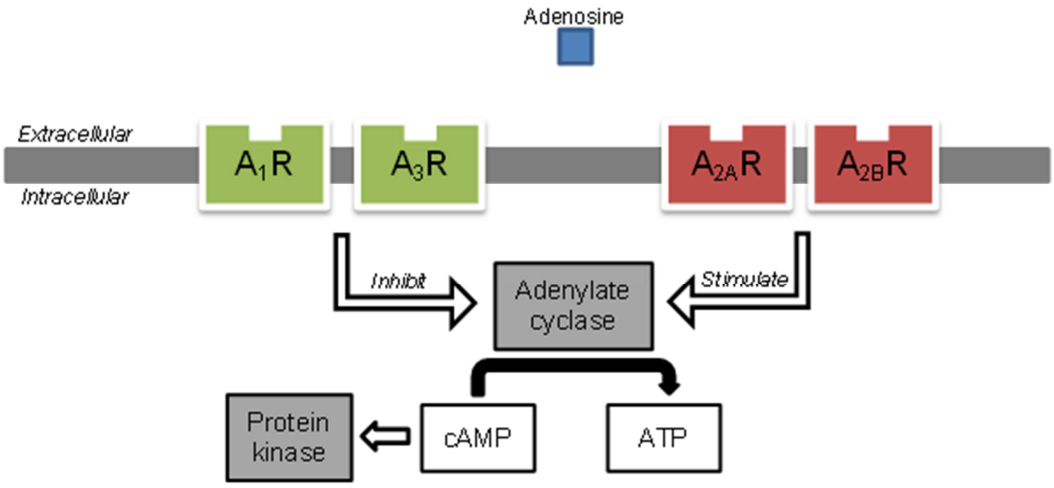

Figure 7. Adenosine receptors intracellular signalling. Binding of adenosine to A_1 and A_3 receptors has an inhibitory function over adenylate cyclase, while activation of adenosine A_{2A} and A_{2B} receptors has the opposite (excitatory) effect. The activity of adenylate cyclase increases the levels of cAMP and, therefore, the activity of protein kinases. cAMP, cyclic adenosine monophosphate; ATP, adenosine triphosphate.

All adenosine receptor subtypes are transmembrane structures coupled to G-proteins. Post-receptor activation signalling differs among receptors and divides them in two groups: A_1 and A_3 receptors couple to inhibitory G proteins ($G_{i/o}$), while A_{2A} and A_{2B} receptors most frequently couple to stimulatory G proteins (G_s) (Fredholm et al., 2005).

Adenosine A_{2A} receptors ($A_{2A}R$) have been shown to bind to more than one G protein. In fact, in the striatum, G_s are rather sparse and, therefore, $A_{2A}R$ is mostly associated with olfactory G proteins (G_{olf}) in that particular region (Kull et al., 2000). The subsequent G-protein signalling is widely described and summarized in fig. 7: A_1R and A_3R inhibit adenylyl cyclase; $A_{2A}R$ and $A_{2B}R$ have the opposite effect (Stiles, 1992; Sperlágh et al., 2007).

1.3.3. Adenosine A_{2A} receptors: distribution, ontogeny and function

In the adult rat brain, $A_{2A}R$ are mostly expressed in the striatum and olfactory bulb. Lower levels have also been detected in the lateral septum, cerebellum, cortex, and hippocampus (Dixon et al., 1996; Svenningsson et al., 1997). At the cellular level, $A_{2A}R$ in the brain can be found in neurons (mostly in postsynaptic sites and dendrites [Hettinger et al., 2001; Rebola et al., 2005]), microglia, astrocytes and blood vessels (Kust et al., 1999; Shin et al., 2000; Nishizaki et al., 2002).

The levels of this particular receptor are not uniform throughout life: the striatum is the only brain region where high levels have been described since gestational day 14 and persist until adult age (Weaver et al., 1993). The intermediate lobe pituitary has a similar but slightly more inconstant profile. Between PND 1 and 7, an ontogenic peek seems to occur due to significant levels in three particular areas: parafascicularis nucleus, locus coeruleus and area postrema. After PND 7, $A_{2A}R$ levels become stable (Weaver et al., 1993). Notably, this pattern is similar in humans and rodents (Fredholm et al., 2001).

$A_{2A}R$ play a role in physiological conditions: for instance, knock-outs for this receptor have an anxiety-like phenotype (Kaster et al., 2015; Fredholm et al., 2005). However, the elimination of $A_{2A}R$ activity through several protocols has revealed to be beneficial (Gomes et al., 2011). A study in which $A_{2A}R$ were genetically depleted presented as result an antidepressant-like phenotype (El Yacoubi et al., 2001). Also related to mood disorders, chronic $A_{2A}R$ blockade reverted the anxious- and depressive-like behaviour of mice subjected to CUS (Kaster et al., 2015). Moreover, blockade of this receptor has partially reverted stress-induced hippocampal modifications, a morphological trait related with depression (Cunha et al., 2006). Accordingly, the opposite manipulation of $A_{2A}R$ – activation – managed to induce memory dysfunction (Cunha et al., 2015). At the structural level, $A_{2A}R$ antagonism has been able to revert the dendritic atrophy presented by stress-impaired animals in the hippocampus, adding a very significant role to these receptors: dendritic branching control (Batalha et al., 2012).

1.3.4. Adenosine A_{2A} receptors in microglia

For the last 10 years, interesting facts have surfaced about the effect of $A_{2A}R$ activation in microglia: activated $A_{2A}R$ stimulate the release of NO (Saura et al., 2005), BDNF (Gomes et al., 2013) and NGF (Heese et al., 1997). Other cytokines and chemokines are affected too, namely TNF-α, chemokine (C-X-C motif) ligand 10 (CXCL10; Newell et al., 2015) and PGE2 (Fiebich et al., 1996). However, the most relevant evidences to this work attribute to $A_{2A}R$ a role in the extension and retraction of microglial processes in response to a stimulus (Orr et al., 2009; Gyoneva et al., 2014). Unperturbed microglia has the capacity to, when sensing the presence of ATP in brain parenchyma, extend its processes towards the site of injury where ATP was released (Davalos et al., 2005). This chemoattraction, however, works differently when microglia is previously stimulated with an inflammatory stimulus, LPS (Orr et al., 2009). This triggers the phenotype commonly described as activated (with increased expression of IL-1β and TNF-α, pro-inflammatory cytokines), which has been associated to the upregulation of $A_{2A}R$ and the downregulation of $P2Y_{12}$ receptors (bind ATP) (Wittendorp et al., 2004; Haynes et al., 2006). These inflammatory-like conditions seem to lead to a process retraction after ATP release (Orr et al., 2009). Importantly, through inhibition of G_s proteins or cAMP it is possible to infer that this $A_{2A}R$-dependent morphological response is dependent on the classical cascade initiated by coupling of ligands to G_s proteins (Orr et al., 2009).

Other perturbations to homeostasis may modulate microglial functions as well (Dai et al., 2010; George et al., 2015). *In vitro*, it has been shown that an increase in glutamate reduces microglia proliferation and increases the extracellular levels of ATP (George et al., 2015). Moreover, it has been observed *in vivo* that the levels of glutamate condition how $A_{2A}R$ will act upon inflammation: within an environment with high levels of glutamate, $A_{2A}R$ will enhance inflammatory reactions, among other deficits caused by traumatic brain injury; low levels of glutamate will evoke the opposite action (Dai et al., 2010). These studies reveal the duality of $A_{2A}R$ in the control of microglia, depending in the basal – physiological or non-physiological – conditions analysed.

1.4. Rationale and aims of the study

As mentioned, *iu*DEX leads to deleterious effects in the CNS, namely neuronal apoptosis and dendritic impairment, accompanied by a phenotype of hyperanxiety and liability to depression. Considering the crucial role of microglia in shaping the brain circuitry, the work hypothesis in this study is that microglia is an important mediator of these alterations and that $A_{2A}R$ are involved in the mechanism (possibly presenting as therapeutic tools). Not only these receptors control the dynamics of microglial processes, they are also involved in the pathophysiology of anxiety and depression, as well as stress-induced dendritic remodelling. The main goals for this work are:

1. Assessing if DEX directly impacts on microglial morphology *in vitro* (cell line) and determining if $A_{2A}R$ blockade is capable of preventing the previous alterations (if existent);
2. Determining the long-term impact of *iu*DEX or chronic $A_{2A}R$ blockade (in adulthood) in the density of $A_{2A}R$ and GR throughout the brain;
3. Determining if $A_{2A}R$ blockade is capable of reverting the previously described effect of *iu*DEX on the morphometry of adult microglial cells in the PFC;
4. Quantifying CORT levels in the blood of adult animals exposed to *iu*DEX and evaluating if $A_{2A}R$ chronic blockade in adulthood is able to alter these levels;
5. Determining the reproductive cycle of the animals, once the study was entirely carried out in females;
6. Correlating both the reproductive cycle and the anxious-/depressive-like phenotype (previously described) of the animals with the respective levels of CORT.

CHAPTER 2

EXPERIMENTAL PROCEDURES

2.1. *In vitro* analysis of microglial N9 cells

2.1.1 Cell culture

The murine microglial cell line N9 (a gift from professor Claudia Verderio from the Neuroscience Institute, Milan, Italy) was grown in Roswell Park Memorial Institute (RPMI, Gibco, Invitrogen, Porto, Portugal) medium supplemented with 5 % heat inactivated fetal bovine serum (FBS; w/v; Invitrogen), 1 % penicillin-streptomycin (w/v; Gibco), 23.8 mM sodium bicarbonate (Sigma, Sintra, Portugal) and 30 mM glucose (Sigma), pH 7.2. The cells were maintained at 37°C under a humidified atmosphere containing 5 % CO_2 and 95 % O_2.

When cell confluence reached approximately 80 % of the flask surface, microglial cells were relocated according to the technique to be performed after pharmacological treatment. Primarily, cells were detached from the 75 cm^2 culture flasks through a trypsinization process using phosphate buffered saline (PBS; 137 mM NaCl [Sigma], 2.7 mM KCl [Sigma], 10 mM $NaH_2PO_4.2H_2O$ [Sigma], 1.8 mM KH_2PO_4 [Sigma] in miliQ H_2O, pH 7.4) with 0.12 % trypsin [w/v, Sigma] and 0.02 % ethylenediamine tetraacetic acid (EDTA; w/v, Sigma), pH 7.4. Trypsin action was inactivated after 5 min with the aforementioned medium due to the serum present in its composition.

Before plating the cells, their concentration was determined using a hemocytometer, a device that allows visualizing and counting cells previously stained with trypan blue (Sigma), a dye not incorporated by viable cells and, thus, allowing to discriminated them. The hemocytometer has four separate quadrants, where the cells are placed under a coverslip. The formula to obtain the number of cells present was:

$$\frac{Number\ of cells}{mL} = \frac{Mean\ of cells}{quadrant} \times dilution factor\ (cells\ in\ trypan\ blue\ ) \times 10^4$$

Cells were plated in 24 well plates at a density of 1×10^4 cells/well (on top of coverslips) in 1 mL of RPMI medium for immunocytochemistry. All plated cells were subjected to a period of 24 h before incubation in order to adhere to the substrate and stabilize. This is quite important once the microglial cell line may become reactive by the culture procedures.

2.1.2. Pharmacological treatment

Four groups of cells were analysed in the *in vitro* experiments: (1) non-treated and treated with (2) DEX (Acros Organics, Geel, Belgium - 230300010), (3) SCH58261 (Tocris, Bristol, UK - 2270), a selective $A_{2A}R$ antagonist, or both (4) DEX and

SCH58261. After the stabilization period, the second and third groups were incubated, respectively, with 1 μM DEX (Caetano, 2014) and 50 nM SCH58261 (Gomes et al., 2013; George et al., 2015). The fourth group was pre-incubated with 50 nM SCH58261 and, 15 min after, with 1 μM DEX.

2.1.3. Immunocytochemistry

After drug incubation, microglial N9 cells on the coverslips were fixed with 4 % paraformaldehyde (PFA, w/v, Sigma) for 20 min at room temperature (RT) and then washed with PBS three times, 10 min each time. Blockade of unspecific binding and permeabilization of the cell membrane to allow the staining of intracellular structures were attained through incubation of fixed cells in a solution of, respectively, 5 % bovine serum albumin (BSA; w/v, Sigma) and 0.1 % Triton X-100 (v/v, Sigma) in miliQ H_2O for 2 h at RT with mild agitation. Cells were incubated with phalloidin (1:500 in PBS, Sigma - P1951), a fungal toxin that binds filamentous actin, for 40 min at RT and, after washing three times with PBS, with 4',6-diamidino-2-phenylindole (DAPI, 1:5000 in miliQ H_2O, Invitrogen - D1306) for 10 min also at RT to stain the nuclei. After new washes, the coverslips were mounted on slides using glycergel mounting medium (DAKO, Glostrup, Denmark - C0563) and dried overnight at 4°C.

2.1.4. Morphological analysis

After loading the images (acquired as described in 2.3) to the ImageJ 1.42 software (developed at the National Institutes of Health, Maryland, U.S.A.), the cell counter plugin was used to attribute to each cell one of the following categories: amoeboid (absence of ramifications) or ramified (with one or more ramifications).

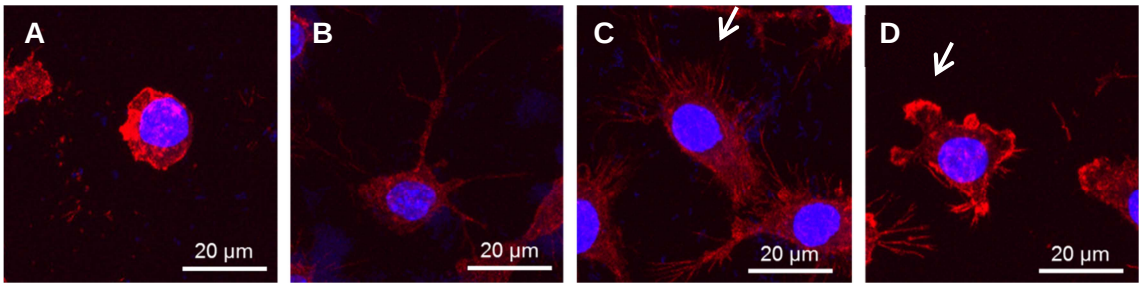

Figure 8. Examples of N9 cells morphologic phenotypes. Microglial N9 cells, (A) amoeboid shaped or (B) ramified, presented themselves with (C) filopodia (white arrow, the filaments surrounding the cell), (D) lamellipodia (white arrow, the protrusions emerging from the cell body), both or, as in (A) and (B), none.

Microglia cell lines are morphologically quite diverse and distinct from the *in vivo* context. Despite being less ramified, the complexity of phenotypes is not diminished. They may present as ramified or amoeboid and, inside of each of these categories, possess or not lamellipodia or filopodia, structures associated with the cell motility (representative images in fig. 8).

Three different forms of analyses were considered (different analysis schematized in table 1). In a first phase, eight categories were considered: in the cell population, amoeboid or ramified cells could have lamellipodia, filopodia, both or none. After concluding the categories were excessive and did not allow for conclusive results, a second approach was attempted, dividing amoeboid or ramified cells according to the presence, or not, of any motile structures. However, cells completely devoided of motile structures were scarse. In summary, the classification according to motility-associated structure was discarded from the analysis because, in last instance, it was the only approach reflecting the culture conditions.

Analysis	**Amoeboid**				**Ramified**			
1	L	F	B	N	L	F	B	N
2	L/F/B		N		L/F/B		N	
3 (Final)	L/F/B/N				L/F/B/N			

Table 1. Different forms of organizing the morphological analysis of N9 cells. Three different categorization systems (1-3) were stablished based on the cell shape (amoeboid or ramified) and on the presence or absence or motility-associated structures. L, lamellipodia; F, filopodia; B, both lamellipodia and filopodia; N, none of the mentioned structures.

2.2. Analysis of biological samples from adult female Wistar rats

This particular set of experiments was conducted using the brains of animals housed and treated in the facilities and with the assistance of researchers from the Life and Health Sciences Research Institute (ICVS, University of Minho). Animals (Wistar rats) were kept at 22°C and 55 % relative humidity in a dark/light cycle of 12 h each (lights turned on at 8:00 am). Food and sterile tap water were available *ad libitum*. Pregnant females were injected subcutaneously with DEX (1 mg/kg) or saline (Sal) at days 18 and 19 of the gestation period. Of the offspring, only the females took part in this study. Of these, some animals (exposed to *iu*DEX or not) were treated for the three last weeks before PND90 with SCH58261 (0.1 mg/kg/day) or Sal via intraperitoneal

injection. During this procedure, animals were sacrificed at three different time points: PND1 (first day of life), PND7 (peak of synaptic formation [Dobbing et al., 1979], microglia expansion [Dalmau et al., 2003], and important ontogenic time point of $A_{2A}R$ [Marangos et al., 1982]) and PND90 (adulthood, where hyperanxiety is observed [Oliveira et al., 2006; Roque et al., 2011]).

The present thesis focuses on the analysis of the animals at PND90, once the other two time points have been previously analysed (Caetano, 2014).

2.2.1. Western blot

Several macro-dissected brain regions were mechanically and chemically digested for Western blot analysis using a tissue homogenizer in a lysis solution containing radioimmunoprecipitation assay buffer (RIPA; 150 mM NaCl, 50 mM trizma [Sigma], 5 mM ethylene glycol tetraacetic acid [EGTA, Sigma], 1 % Triton X-100 [v/v], 0.5 % deoxychlolic acid [DOC; w/v, Sigma], 0.1 % sodium dodecyl sulfate [SDS; w/v; Bio-Rad Laboratories, Hercules, CA, USA] in miliQ H_2O, pH 7.5) and 1 mM dithiothreitol (DTT, Sigma) supplemented with complete miniprotease inhibitor cocktail tablets and phosphatase inhibitors (Roche, Penzberg, Germany), in order to avoid protein degradation during the extraction process by such enzymes. The homogenates were then centrifuged at 13 200 rotations per minute (rpm) for 10 min at 4°C to remove cells components other than protein such as nuclei, lysosomes, mitochondria or even whole cells – those remain in the pellet and are excluded. The supernatant was saved for the analysis of the levels of proteins (GR and $A_{2A}R$) through Western blot.

The bicinchoninic acid (BCA) protein assay was performed afterwards with the purpose of determining the concentration of total protein in each sample in order to run a fixed amount of total proteins between samples (Smith et al., 1985). The assay is based on the reduction of copper ions by peptide bonds from Cu^{2+} to Cu^{+} (biuret reaction, temperature-dependent). The latter forms a complex with the BCA characterised by a strong absorbance at 562 nm (purple). Therefore, the absorbance of a sample is positively correlated with protein concentration, here assessed with the Pierce™ BCA Protein Assay Kit (Thermo-Scientific, Waltham, Massachusetts, USA). The standard concentration curve was made up of known concentrations of BSA diluted in the lysis buffer and miliQ H_2O (1:20). The samples were also diluted in miliQ H_2O (1:20). After addition of the reagents from the BCA kit, the 96 well plate was kept in the incubator for 30 min at 37°C, followed immediately by a read of the absorbance at 570 nm.

Once determined the protein concentration of each sample, they were normalized to a common concentration, to facilitate gel loading and avoid interferences in the electrophoresis. This normalization was achieved by adding volumes of miliQ H_2O and sample buffer 6× (70 % trizma-HCl [0.5 M, pH 6.8], 30 % glycerol [v/v, Sigma], 10 % SDS [w/v], 0.6M DTT, 0.012 % bromophenol blue [w/v, M&B, Mumbai, India], diluted in miliQ H_2O) that would decrease its concentration to 1×. Denaturation took place at 70°C for 5 min. Both sample buffer and heat exposure are necessary to denature proteins and expose their epitope – the structure to which the antibody will bind.

In order to begin the sodium dodecyl sulfate polyacrylamide gel electrophoresis (SDS-PAGE) the processed samples were then loaded onto the stacking gel (4 % bisacrylamide [v/v, Bio-Rad], trizma-HCl [0.125, M pH 6.8], 10 % SDS [w/v], 10 % ammonium persulfate [APS, w/v, Sigma], 2 % N,N,N',N'-tetramethylethylenediamine [TEMED, v/v, Bio-Rad]). The resolving gel (8 % bisacrylamide, trizma-HCl [0.375 M, pH 8.8], 10 % SDS [w/v], 10 % APS [w/v], 1 % TEMED [v/v]) had the same pore size in every conducted electrophoresis (GR, 95 kDa; $A_{2A}R$, 45 kDa and glyceraldehyde 3-phosphate dehydrogenase [GAPDH], 37 kDa), given that 8 % bisacrylamide is adequate for detection of proteins that weight between 25 and 200 kDa.

Separation of proteins in a bicine-buffered solution (25 mM trizma, 25 mM bicine [Sigma], 0.1 % SDS [w/v], pH 8.3) occurred in two phases: at 60 V for 15 min and at 150 V for 1 h, both at RT. Meanwhile, polyvinylidene difluoride (PVDF) membranes (Millipore, Billerica, Massachusetts, USA) were activated at RT through sequential immersions in: methanol (Sigma) for 30 s, distilled H_2O for 5 min and, finally, in electrotransfer buffer (10 % methanol [v/v, Sigma] in 3-[cyclohexylamino]-1 propane sulfonic acid [CAPS, Sigma], pH 11) for 5 min.

Once ended the electrophoresis, the proteins distributed in the gel were transferred to the activated membranes at 0.75 A for 1 h and 30 min (4°C) in electrotransfer buffer, using mild agitation.

Membranes were blocked, in order to prevent unspecific binding of antibodies, in a mildly agitated solution of 5 % low-fat dry milk (w/v) diluted in tris-buffered saline with tween 20 (TBS-T; 20 mM trizma, 137 mM NaCl, 0.1 % tween-20 [v/v; Merck, Darmstadt, Germany] diluted in miliQ H_2O, pH 7.6) for 1 h at RT.

All antibody (for full description, see table 2) dilutions were prepared in 1 % low-fat dry milk diluted in TBS-T. Membranes were incubated with the primary antibodies overnight at 4°C and then washed three times, 10 min each time, with TBS-T at RT.

Incubation with alkaline phosphatase-conjugated secondary antibodies took place for 1 h at RT.

Antibody	Loading (µg)	Supplier	Host	Type	Dilution
anti-$A_{2A}R$	60 - 150	Santa Cruz Biotechnology (sc-3226)	Mouse	Monoclonal	1:200
anti-GR	25	Santa Cruz Biotechnology (sc-1004)	Rabbit	Polyclonal	1:1000
anti-GAPDH	-	Abcam (ab9485)	Rabbit	Polyclonal	1:1000
anti-Mouse	-	BioRad (#170-6516)	Goat	IgG	1:5000
anti-Rabbit	-	GE Healthcare (NIF1317)	Goat	IgG	1:10000

Table 2. List and respective description of the antibodies used for Western blot.

Membranes were once again washed and incubated with enhanced chemofluorescent (ECF; GE Healthcare) or up to 5 min at or with enhanced chemofluorescent (ECL). ECF and ECL are substrates to alkaline phosphatase and horseradish peroxidase, respectively, resulting in a product detectable in the reaction spot, therefore locating the protein of interest. The detection of fluorescence was carried out on an Thyphoon FLA 9000, GE Healthcare (ECF) or ImageQuant™ LAS 500, GE Healthcare (ECL).

To correctly assess the variations on the content of a particular protein, all membranes were re-probed for anti-GAPDH, a protein that is not affected by the pharmacological treatment (rabbit polyclonal anti-GAPDH; 1:1000; Abcam, Cambridge, UK – ab9485). In order to do so, membranes were washed to remove the ECF and immersed, sequentially, in methanol for 10 s and distilled H_2O for 5 min. Blockade was also repeated in the aforementioned solution for 30 min. The rest of the protocol was exactly as described above. The immunoreactivity of the obtained bands was quantified and normalized to the detected amounts of GAPDH using ImageQuant 5.0 software (Molecular Dynamics, Inc., Sunnyvale. CA, USA)

2.2.2. Immunohistochemistry

Adult rat brains were sliced using a cryostat (Leica CM3050S, Nussloch, Germany) set at -21°C as chamber temperature and -19°C as object temperature. For that purpose,

brains were completely involved in optimal cutting temperature (OCT, Shandon Cryomatrix, Shandon, USA) compound and, after solidified, aligned in the cutting platform. The obtained coronal slices, 50 µm thick, were collected and transferred to a 24 well plate where they were kept in cryoprotection solution (50 mM $NaH_2PO_4.H_2O$, Merck], 50 mM K_2HPO_4 [Sigma], 30 % sucrose [w/v, Sigma] 30 % ethylene glycol [v/v, Sigma], diluted in miliQ H_2O, pH 7.2). The slices were stored at -20°C until further manipulation.

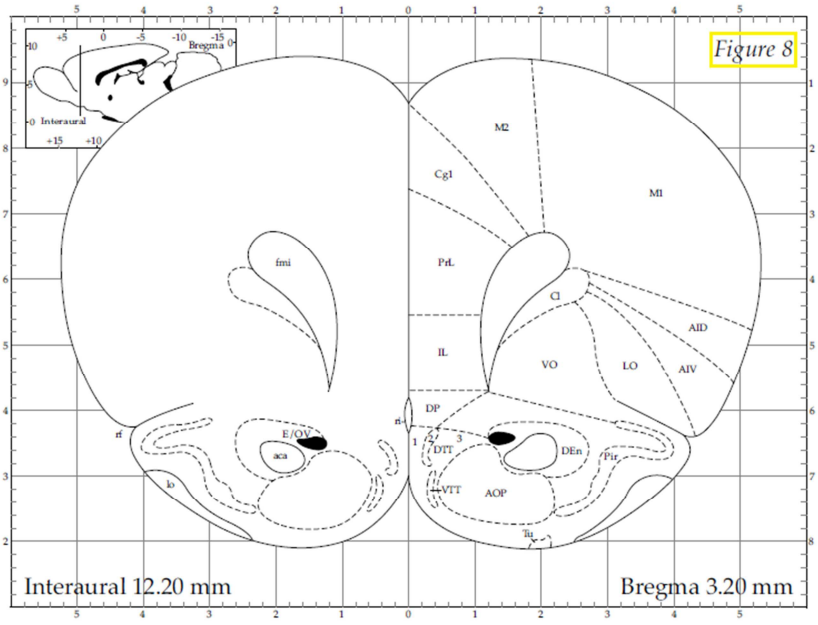

Figure 9. Brain localization and representation of slices from the prefrontal cortex. Brain slices used for immunohistochemistry were retrieved from the PFC, with the appearance and stereotaxic coordinates indicated in the image (Paxinos and Watson, 1998).

Immunodetection was carried out on the 50 µm free-floating slices previously prepared. According to Paxinos and Watson, 1998, the selected slices were located at the stereotaxic coordinates of interaural 12.20 mm and bregma 3.20 mm. The choice of these particular coordinates is justified by the privileged perspective on the PFC, illustrated in fig. 9.

Primarily, sections were washed three times with PBS, 10 min each time, in mild agitation. Blockade of unspecific binding and permeabilization of the cell membrane to allow the staining of intracellular structures were attained through incubation of fixed cells in a solution of, respectively, 5 % BSA (w/v) and 0.1 % Triton X-100 (v/v) in miliQ H_2O for 2 h at RT with mild agitation. Antibodies were prepared in this same solution (for full description, see table 3).

Antibody	Supplier	Host	Type	Dilution
anti-Iba-1	WAKO (019-19741)	Rabbit	Polyclonal	1:1000
anti-Rabbit	Invitrogen (A21206)	Donkey	IgG	1:1000

Table 3. List and respective description of the antibodies used for immunohistochemistry.

Incubation of slices with the primary antibody took place for 48 h at 4°C. Ionized calcium-binding adapter molecule 1 (Iba-1) is a cytoplasmic microglia/macrophage-specific calcium-binding protein (Ito et al., 1998). After new washes, sections were incubated with the secondary antibody for 2 h at RT along with moderate agitation before being once again washed three times. Negative controls (incubation with blocking solution instead of the primary antibody) were made in parallel to ensure the selectivity of the secondary antibody. Then, slides were incubated, also while mildly agitated, with DAPI (1:5000) for 10 min at RT and washed with PBS. Finally, coverslips were mounted over the sections on gelatinized microscope slides using DAKO glycergel mounting medium and allowed to air dry overnight. After sealing the coverslips with transparent nail polish, the slides were kept in a dark environment at 4°C.

The main goal of this project was the assessment of microglial processes, as detailed as possible. To achieve such minuteness, the Neurolucida software (MBR Biosciences) was chosen to this task. Even though it was initially conceived to reproduce the structure of neurons, an optimization allowed its use for microglia reconstruction and morphometric analysis (Hinwood et al., 2012; Caetano, 2014).

After importing the Z-stacks to the software, every cell was manually drawn as it progressed or regressed along the several acquired planes, granting a three-dimensional image of each cell as an outcome. For each individual, 10 cells were reconstructed in the sets of animals untreated or treated with DEX (re-analysed groups). For the sets of animals treated with SCH58261 or DEX and SCH58261, 15 cells were analysed (first analysis).

Once obtained the contours of the cell body, the criterion established for the reconstruction of the processes was that all ramifications, regardless their length, should be taken into consideration, so that the final result was as similar as possible to the original cell.

After drawing each cell, morphometric data (branched structure analysis and Scholl analysis) was extracted by the Neurolucida Explorer, an extension of the software. Scholl analysis does not divide processes by orders but by radius - concentric circles are drawn around the cells body each 10 µm (fig. 10). Even though several results become available, the main focus of the present analysis is the number and length of microglial ramifications.

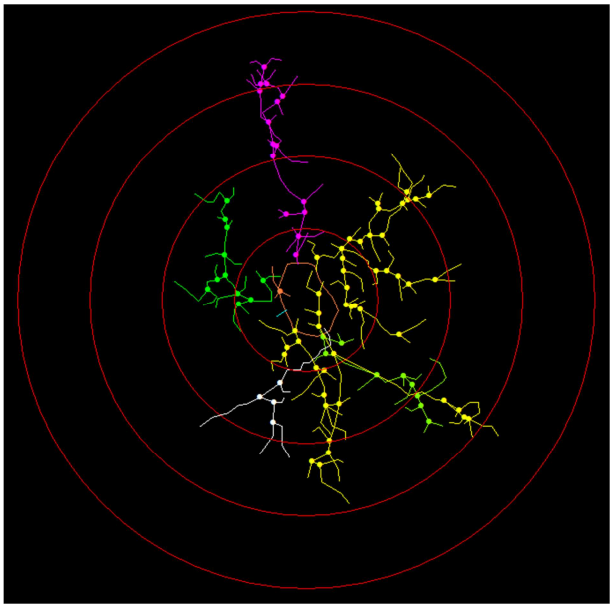

Figure 10. Example of Scholl analysis applied to a microglial cell. After optimizing Neurolucida for analysis of microglial cells, it is possible to carry out Scholl analysis through the Neurolucida Explorer. The red lines are concentric circles around the cell body every 10 µm. Length and number of branches is assessed according to the number times they intersect every circle, instead of the order.

2.3. Estrous cycle analysis

The estrous cycle is the reproductive cycle of rats. It is short (4-5 days), ergo a good model for the study of changes occurring during this cycle, which is characterized, like in humans, by the oscillations in the hormonal levels, such as estrogen (Caligioni, 2009).

The stage of the estrous cycle corresponding to the female adult rats of this study was assessed according the literature on this subject (Marcondes et al., 2001; Westwood, 2008; Caligioni, 2009; Byers et al., 2012). It can be divided into four different stages, depending on the prevalence of each cell type in the smear. There are three cell types to be observed in these preparations that are, visually, quite simple to distinguish: nucleated epithelial cells (relatively round and nucleated), cornified epithelial cells

(irregularly shaped and anucleated) and leukocytes (very much smaller than the other two and nucleated). The four stages are:

Proestrus: significant prevalence of nucleated epithelial cells, clustered or individually, with possible occasional presence of the other two types (fig. 11A);

Estrus: almost exclusively cornified epithelial cells are present (fig. 11B);

Metestrus: in this stage, even though the percentage of leukocytes is slightly higher, nucleated and cornified epithelial cells are present almost in the same amount as the first (fig. 11C);

Diestrus: even though nucleated and cornified epithelial cells may be observed, in this stage leukocytes are visibly predominant (fig. 11D).

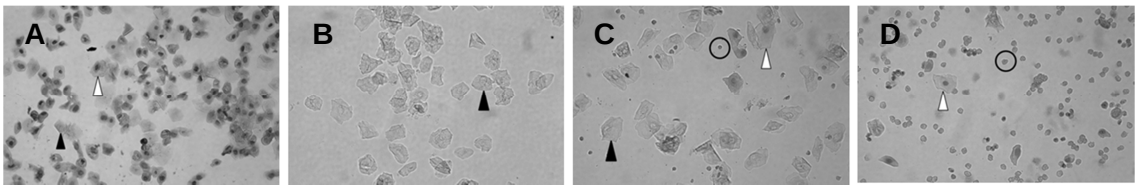

Figure 11. The four stages of the estrous cycle. Three types of cells may be distinguished: leukocytes (circle), cornified epithelial (black arrow) and nucleated epithelial (white arrow). The four stages are separated according to predominance of each cell: (A) proestrus – nucleated epithelial; (B) estrus – cornified epithelial; (C) Metestrus – approximately the same amount of all types; and (D) diestrus – leukocytes (Byers et al., 2012).

The smears were obtained through vaginal smear cytology, previously performed at ICVS, as explained. Staining was performed using the haematoxylin and eosin method (Marshall et al., 1983). Females considered in this analysis were 90 days old.

2.4. Corticosterone determination

Samples from rats at PND 90 were collected at 8:00 am (start of the less active period in rats) and 8:00 pm (beginning of the more active period, peaking at this hour) through puncture of the tail vein. Quantification of the steroid was carried out using the Corticosterone ELISA Kit (Abcam). Blood samples or known concentrations of CORT (for the standard concentration curve) were added to a 96 well plate coated with antibody against CORT, before adding biotynilated CORT (a second antibody). After five washes, the streptavidin-peroxidase conjugate was also added, followed by new washes. The chromogen substrate was loaded to obtain the blue colour formed by the reaction with the previous reagent. After waiting 20 min, the reaction was stopped with hydrochloric acid, followed immediately by a read of the absorbance at 450 nm.

2.5. Image Acquisition

The images were acquired with a laser scanning confocal microscope LSM 710 META connected to ZEN software (Zeiss, Germany).

For *in vitro* studies, 10 images of microglial cells stained with phalloidin were randomly obtained from each duplicate of every separate experiment by a 63x objective lens (oil immersed, Plan-Apochromat 63x/1.40 Oil DIC M27).
Regarding brains, for the slices of each individual, images were acquired of 10-15 random microglial cells stained with both DAPI and Iba-1 within the PFC region using a 63x objective (oil immersed). The high magnification is here needed to provide enough resolution for a correct morphometric assessment later on. Settings were optimized so that the labelling with Iba-1 becomes as evident as possible in microglial processes, the structures of main interest to the project, and kept throughout the all sets of acquisitions. To ensure that the images being acquired belonged to the correct region, one image for each individual was also acquired with a 20x objective lens (Plan-Apochromat 20x/0.8 M27, data not shown).

2.6. Statistical analysis

The statistical analysis was carried out in GraphPad Prism version 5. All graphic values are expressed as mean ± standard error of the mean (SEM). Comparison between two independent means was done by a Student's t test. To assess differences between four groups, a one-way analysis of variance (ANOVA) was used, followed by a Tukey's post hoc test, to compare all groups to each other. Differences were considered significant at (*) $p<0.05$, (**) $p<0.01$ and (***) $p< 0.001$. All statistical analysis was performed using absolute values.

In order to assess if the levels of circulating CORT were correlated with the quantification of anxious or depressive-like animals (positive- or negatively), the Pearson correlation coefficient test was performed. This test is designed to assess the strength of the inter-variation of values, by applying the following formula:

$$P = \frac{n(\sum xy) - (\sum x)(\sum y)}{\sqrt{(\sum x^2 - (\sum x)^2)(\sum y^2 - (\sum y)^2)}}.$$

In this particular analysis, CORT levels correspond to the "x" variable; "y" values are the measurements of performances in behavioural tests.

The result of the Pearson (P) correlation coefficient is a value ranging from -1 to 1. A result where P=1 means that the two variables are positively correlated (which does

not necessarily means causation); on the other hand, P=-1 indicates that these variables are negatively correlated. The result in between these numbers, P=0, expresses the absence of any correlation between the compared measurements. Differences were considered significant at $p < 0.05$.

Behavioural tasks were performed with the assistance of the ICVS research team. For evaluating anxiety-related behaviour, an elevated plus maze (EPM) test was adopted. This test consisted of placing the animal on an elevated platform with four arms (two open and two closed). The longer the animal stays in either of the closed arms (as opposite to the open arm [OA]), the less exploratory behaviour it displays, presenting therefore with anxiety-related behaviour. The employment of the forced swimming test (FST) allowed for the assessment of depressive like-behaviour. In this test, the animal is put inside a glass cylinder filled with water. Once rodents avoid water, the rat will try to swim in order to escape; the faster the rat quits swimming, the more depressive-like behaviour it presents with. Latency to immobility consists of the period of time the animal keeps swimming. The immobility to total time ratio is informative of how long the animal remains still. Both measurements complete each other (Sousa et al., 2006).

CHAPTER 3

RESULTS

3.1. *In vitro* analysis of microglial N9 cells

Recently, is has been shown that microglia is morphologically altered in animals exposed *iu*DEX (less and shorter processes) and, very importantly, that these alterations are already present during crucial stages of neurodevelopment and synapse formation – PND1 and PND7 (Caetano, 2014). This study was based on the morphometric analysis of cells from brain slices. Despite the advantage of the physiological context, microglial cells are not isolated. Therefore, the aforementioned phenotypic modifications may arise not from the direct effect of DEX on microglia, but from the reaction of these cells to other environmental elements. So, *in vitro* analyses were conducted to investigate if microglial cells were phenotypically altered directly by DEX.

3.1.1. Characterization of cultured microglia

The analysis of cultured microglia (N9 mouse microglial cell line) in the present work revealed that these cells are quite different from the brain parenchyma (fig 12 and fig. 14). In the first context, microglia are much less ramified; still, complex phenotypes were found. As explained in the experimental procedures, initially two factors were considered to stablish a categorization system: the presence of ramifications and the existence of structures associated to motility. Filopodia or lamellipodia (actin filaments with different structural assemblies) were observed in cultured microglia. Amoeboid and ramified cells were found to possess lamellipodia, filopodia or both. Situations were observed where neither was present, but rarely. Because motile structures were not considered to reflect the qualitative results from the detailed morphological analysis of the samples, classification of cell morphology focused exclusively on the cell shape: amoeboid or ramified. In conclusion, although the importance of studies in cultured microglial cells is indisputable, one must keep in mind the limitations of these same studies because of the clear differences found when compared to microglia in brain slices and the confounding effect of multiple cellular morphologic presentations.

3.1.2. Dexamethasone effects on microglial morphology

N9 cells were cultured and exposed to DEX 1 μM for 24 h, an experimental protocol optimized by Caetano, 2014. After immunocytochemistry (staining with fluorescent phalloidin), the morphology of cells was analysed using images acquired in the confocal microscope. The ramified to amoeboid cells ratio was increased by DEX comparing to non-treated conditions (0.8 ± 0.2, $p>0.05$, compared to non-treated

conditions [0.5 ± 0.2]; fig. 12I), representing an increase of the percentage of ramified microglia within the culture in the presence of DEX.

3.1.3. Adenosine A_{2A} receptors modulation of dexamethasone effects on microglial morphology

Because $A_{2A}R$ are plausible candidates for the mediation of microglial alterations induced by DEX, cells were exposed to SCH58261 50 nM (a concentration at which it works as a selective inhibitor of $A_{2A}R$) or pre-incubated with SCH58261 50 nM for 15 min before exposure of cells to DEX 1 μM (24 h).

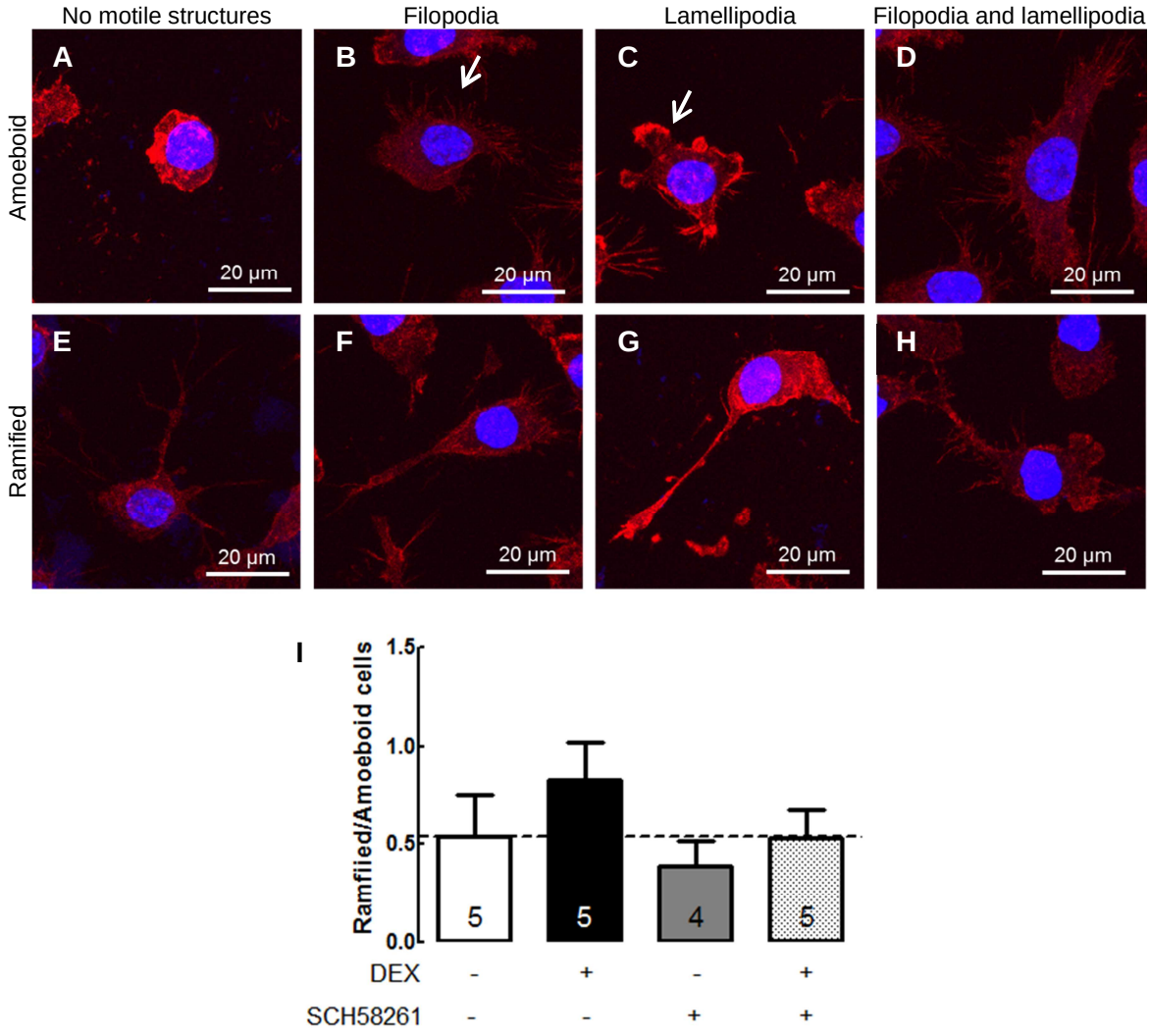

Figure 12. Effect of dexamethasone and/or adenosine A_{2A} receptors blockade on the morphology of N9 microglial cells. Cells were treated with (+) or without (-) DEX 1 μM in the presence and in the absence of SCH58261 ($A_{2A}R$ antagonist) 50 nM for 24h. When together, SCH58261 was added to the cells 15 min before DEX, incubating for 24 h as well. Then, cells were fixed for immunocytochemistry. The diversity of morphological phenotypes (regarding shape and motile structures) is attested by the representative images of phalloidin-stained microglia: Amoeboid or ramified microglia may have **(A, E)** no motile structures, **(B, F)** filopodia – white arrow, **(C, G)** lamellipodia – white arrow

or **(D, H)** both**. (I)** Bars represent the ramified to amoeboid cells ratio within cell culture. Results are expressed as mean ± standard error of the mean (SEM) of 4-5 independent experiments (one-way ANOVA).

The blockade of $A_{2A}R$ before adding DEX exhibited a tendency to prevent the alterations previously observed by the incubation with DEX. The values of the ramified to amoeboid cells ratio was brought back to control levels (0.5 ± 0.1, $p>0.05$, compared to non-treated conditions; fig. 12I).

3.2. Analysis of biological samples from adult female Wistar rats

3.2.1. Impact of dexamethasone and chronic adenosine A_{2A} receptors blockade on the density of glucocorticoid and adenosine A_{2A} receptors

To study the crosstalk between the synthetic GC DEX and $A_{2A}R$, several brain regions were scanned for alterations in the density of the respective receptors.

Brain areas displayed in this analysis were elected by their potential involvement in the regulation of the HPA axis or in the pathophysiology of mood disorders: amygdala (Amy), dorsal dentate gyrus (dDG), ventral dentate gyrus (vDG), dorsal hippocampus (dHIP), ventral hippocampus (vHIP), NAcc, PFC and striatum (Str). The results of work preceding the present thesis show that animals treated with *iu*DEX have alterations in A_1R, $A_{2A}R$ and GR levels in the first post-natal week (Caetano, 2014).

Brain regions from animals at PND90 (3 months old) were processed for Western blot in order to evaluate the levels of GR and $A_{2A}R$ in a long term scenario. GR and $A_{2A}R$ densities were quantified in four experimental groups: Sal, *iu*DEX, SCH58261 in adulthood and *iu*DEX followed by SCH58261 in adult age. As quantified in fig. 13 and summarized in table 4, the administration of *iu*DEX and the subsequent chronic administration of SCH58261 in adulthood, as well as the chronic administration of SCH58261 without previous exposure to *iu*DEX, induced alterations in the density of $A_{2A}R$ and GR, which depend on the brain region analysed.

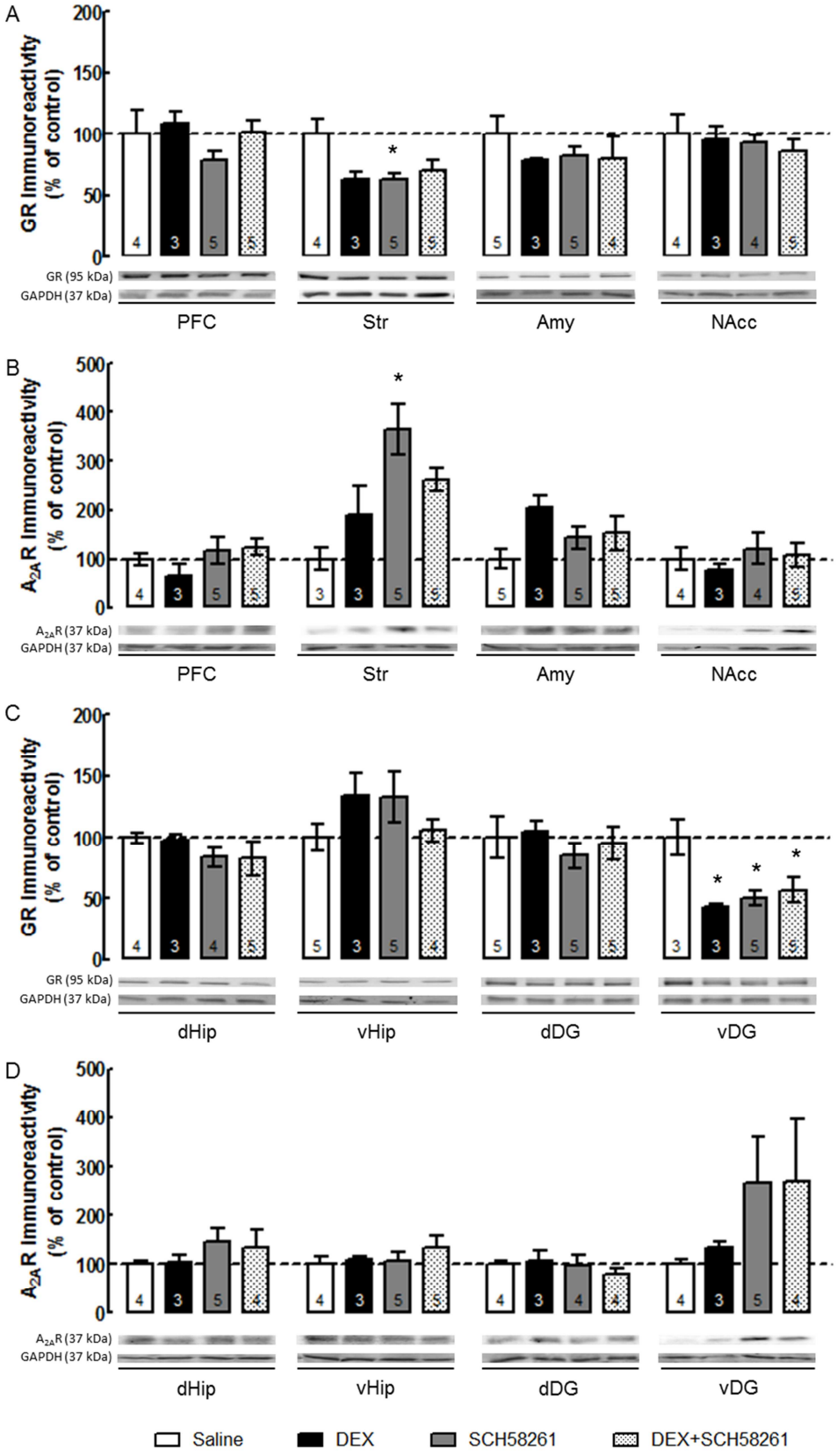

Figure 13. Impact of dexamethasone and/or adenosine A_{2A} receptors blockade on the density of glucocorticoid and adenosine A_{2A} receptors in several brain regions. Pregnant females were injected with DEX (1 mg/kg sc) or Sal

during pregnancy (ED 18 and 19). At adulthood, animals from both groups were injected with SCH58261 (0.1 mg/kg ip) or Sal for 3 weeks before PND90. At PND90, animals were sacrificed and brains were dissected, lysed and homogenised for western blot in order to detect and quantify **(A, C)** GR (90-95 kDa) and **(B, D)** $A_{2A}R$ (45 kDa). Results are expressed as mean ± SEM of 3-5 animals (*p<0.05, compared with control conditions using the Tukey's multiple comparison test). For each condition of each region, a representative blot is presented, including the protein to be detected and GAPDH (37 kDa), the loading control. PFC, prefrontal cortex; Str, striatum; Amy, amygdala; NAcc, *nucleus accumbens*; dHip, dorsal hippocampus; vHip, ventral hippocampus; dGD, dorsal dentate gyrus; vDG, ventral dentate gyrus.

Brain region	DEX (n=3-5)[1]		SCH58261 (n=3-5)[1]		DEX+SCH58261 (n=3-5)[2]	
	GR	$A_{2A}R$	GR	$A_{2A}R$	GR	$A_{2A}R$
PFC	108.1 ± 9.7	66.1 ± 23.7	79.1 ± 6.1	116.4 ± 27.5	101.7 ± 9.3	124.7 ± 17.5
Str	63 ± 6.2	189.4 ± 61.8	↓ **62.7 ± 5.2**	↑ **365.5 ± 51.6**	70.1 ± 9	262.8 ± 24.4
Amy	78.5 ± 1.3	205.5 ± 24.1	82.5 ± 7.4	144.3 ± 23.1	79. 2 ± 18.9	153 ± 33.9
NAcc	95.2 ± 10.9	78.9 ± 10.4	93.6 ± 5.2	121.9 ± 32	85.9 ± 9.8	109 ± 25
dHip	97.7 ± 4.9	104.5 ± 15.6	84.3 ± 7.7	145.9 ± 28.3	82. 9 ± 13.6	133.4 ± 37.6
vHip	133.5 ± 18.7	109.9 ± 5	132.6 ± 20.2	107.9 ± 17	105. 5 ± 9.1	135.7 ± 23.5
dDG	105.4 ± 8.1	108 ± 21	82.2 ± 10.4	97.6 ± 20.3	95.4 ± 13	80.7 ± 11.5
vDG	↓ **43 ± 3.2**	134.9 ± 10.1	↓ **50.3 ± 6.1**	266.9 ± 92.5	↓ **56.9 ± 10.3**	270.4 ± 125.4

Table 4. Summary of changes in the density of glucocorticoid and adenosine A_{2A} receptors in the brain. Effects of different treatments on the density of GR and $A_{2A}R$ in several brain areas, presented as percentage of control. Grey and blue areas represent statistically significant changes in the levels of GR and $A_{2A}R$, respectively. [1]Compared with Sal-treated animals. [2]Compared with DEX-treated animals. PFC, prefrontal cortex; Str, striatum; Amy, amygdala; NAcc, *nucleus accumbens*; dHip, dorsal hippocampus; vHip, ventral hippocampus; dGD, dorsal dentate gyrus; vDG, ventral dentate gyrus.

3.2.2. Morphometric analysis of microglial cells in the prefrontal cortex

For this task, the brains of animals at PND90 subjected to different treatments were cryosectioned and stained with Iba-1 (microglial marker) through immunohistochemistry. Acquisition of images using a confocal microscope allowed for the stacking of all the planes of each microglial cell, leading to a 3D reconstruction in the Neurolucida software, accurately informative of the cell morphometric profile.

3.2.2.1. Dexamethasone effects on microglial morphometry

Validation of previous results (Caetano, 2014) to eliminate interpersonal differences in morphometric analysis confirmed that the exposure of animals to *iu*DEX affects

microglia morphology, not only during crucial steps of neurodevelopment (Caetano, 2014) but also later in life (present results).

Regarding the number of ramifications, a significant decrease was observed in processes belonging to order 6 of animals exposed to *iu*DEX. This result is consistent with previous analyses that report the same effect, as well as the global tendency for decrease in the number of processes of practically all orders (Caetano, 2014).

The length of processes was globally diminished by DEX, an effect particularly clear in order 6 (fig. 14R).

Scholl analysis did not show any differences with reference to number (fig. 14S) or length (fig. 14T) of processes between control and DEX-treated animals. The numeric results associated with the morphometric analysis are summarized in table 5.

3.2.2.2. Chronic adenosine A_{2A} receptors blockade effects on microglial morphometry

Chronic administration of a selective $A_{2A}R$ antagonist in adulthood through administration of SCH58261, *per se*, decreased the number of processes in microglial cells belonging to the orders 4 to 10 (fig. 14Q).

The length was also significantly decreased by SCH58261 administration from orders 2 to 10 (fig. 14R).

Scholl analysis revealed a significant decrease in the number of intersections between radius 20 and 50 (fig. 14S). According to this particular analysis, the length of ramification was decreased as well at the same set of radius (fig. 14T). The numeric results associated with the morphometric analysis are summarized in table 5.

3.2.2.3. Impact of dexamethasone and chronic adenosine A_{2A} receptors blockade on microglial morphometry

Confronting the morphometry of PFC microglia exposed to DEX and SCH58261 or exposed to DEX alone, marked differences are also detectable. In terms of ramifications per order, in animals treated with the GC and the antagonist, this number significantly lowers in orders 3 to 10 (fig. 14Q). The exact same orders have lower length of processes (fig. 14R). Scholl analysis indicated that the number of intersections is decreased in radius 20, 30 and 40 (fig. 14S). Furthermore, length is also diminished between radius 20 and 50 (fig. 14T). The numeric results associated with the morphometric analysis are summarized in table 5.

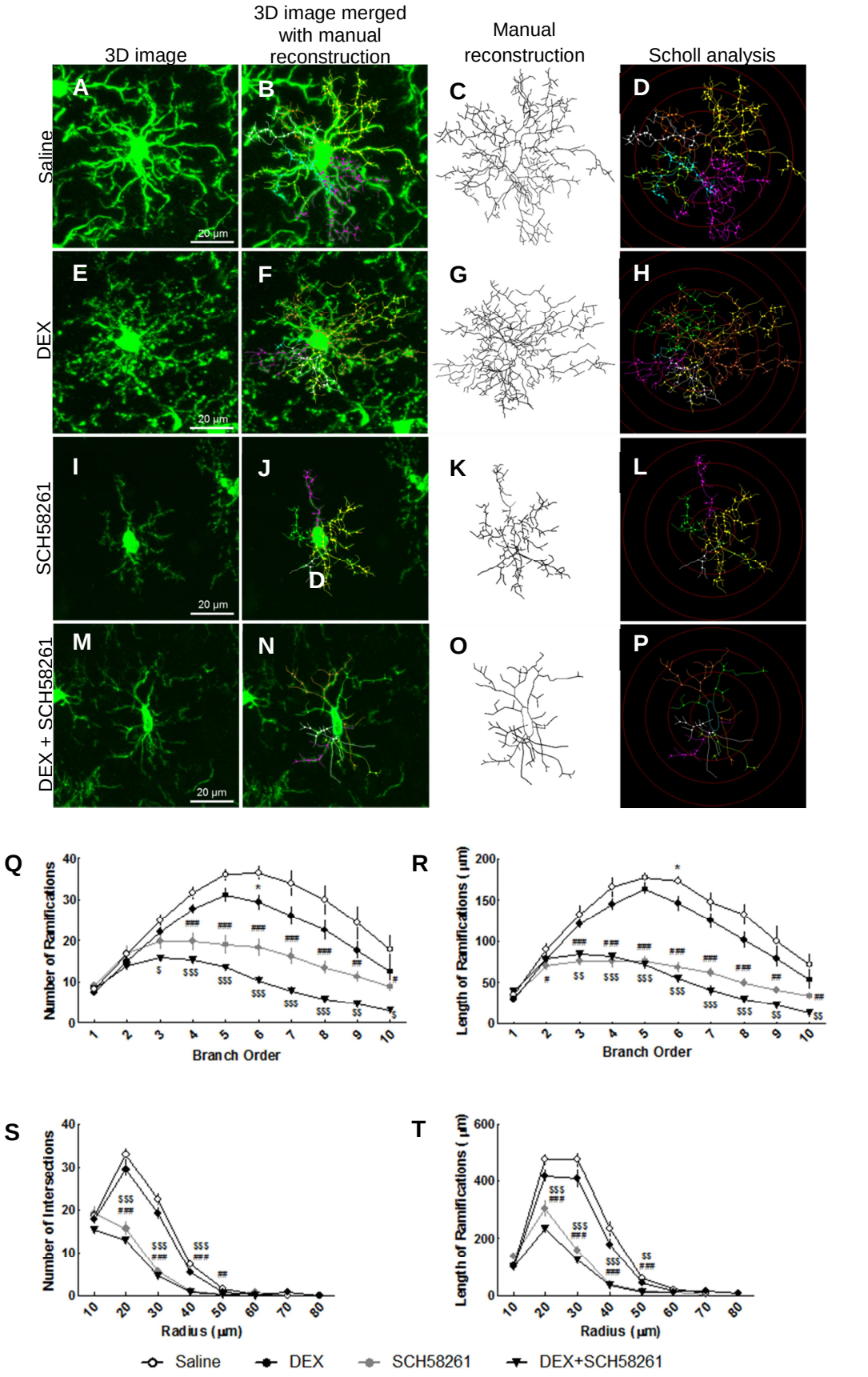

Figure 14. Effect of dexamethasone and/or adenosine A_{2A} receptors blockade on the number and length of microglial processes located in the prefrontal cortex. Pregnant females were injected with DEX (1 mg/kg sc) or Sal

during pregnancy (ED 18 and 19). At adulthood, animals from both groups were injected with SCH58261 (0.1 mg/kg ip, $A_{2A}R$ antagonist) or Sal for 3 weeks before PND90. At PND90, animals were sacrificed and brains were removed and cryosectioned. **(A-P)** Immunohistochemistry labelled microglia with Iba-1 from the PFC, providing accurate images of all the planes each cell is found on. The resulting 3D picture was used as the basis of the three-dimensional reconstruction of these cells in the Neurolucida software. Morphometric data were extracted from the reconstructions with the Neurolucida Explorer regarding the **(Q)** number and **(R)** length of the processes and, similarly, the **(S)** number and **(T)** length of the intersections of processes and radius considered in the Scholl analysis. Results are expressed as mean ± SEM of 6-7 animals. (*p<0.05, comparing DEX treatment with control conditions using the Tukey's multiple comparison test; $^{\#}$p<0.05, $^{\#\#}$p<0.01, $^{\#\#\#}$p<0.001, comparing SCH58261 treatment with control conditions using the Tukey's multiple comparison test); ($^{\$}$p<0.05, $^{\$\$}$p<0.01, $^{\$\$\$}$p<0.001, comparing DEX and SCH58261 with DEX treatments using the Tukey's multiple comparison test).

Branch Order	Saline (n=6)		DEX (n=6)[1]		SCH58261 (n=7)[1]		DEX+SCH58261 (n=7)[2]	
	Number	Length (µm)	Number	Length (µm)	Number	Length (µm)	Number	Length (µm)
1	8.2 ± 0.3	35.3 ± 3.7	7.3 ± 0.3	29.9 ± 1.6	9.2 ± 0.8	32.2 ± 2.1	8.2 ± 0.3	39.2 ± 3.1
2	16.6 ± 0.6	90.6 ± 6	14 ± 0.5	78.9 ± 3.7	16.9 ± 1.7	**↓ 70 ± 5.2**	13.9 ± 0.5	78.1 ± 4.4
3	24.9 ± 1.2	132.2 ± 11.2	22.1 ± 1	121 ± 5.8	19.9 ± 2	**↓ 76.5 ± 6**	**↓ 15.7 ± 0.4**	**↓ 84.2 ± 4.5**
4	31.6 ± 1.5	166.5 ± 11.1	27.8 ± 1.1	144.7 ± 7.4	**↓ 19.7 ± 2.1**	**↓ 75.4 ± 7.3**	**↓ 15.2 ± 0.3**	**↓ 81.4 ± 4**
5	36 ± 1.2	177.2 ± 6.1	31.1 ± 1.7	163.9 ± 6.6	**↓ 18.9 ± 2.2**	**↓ 75.5 ± 5.6**	**↓ 13.4 ± 0.7**	**↓ 71.7 ± 3.9**
6	36.5 ± 1.6	173.4 ± 4.8	**↓ 29.3 ± 1.8**	**↓ 146.1 ± 9.1**	**↓ 18.2 ± 2.2**	**↓ 68.4 ± 6.7**	**↓ 10.3 ± 0.9**	**↓ 55.2 ± 4.3**
7	33.9 ± 2.9	148.4 ± 10.8	26 ± 2.3	125 ± 9.2	**↓ 16.1 ± 2**	**↓ 61.8 ± 5.5**	**↓ 7.8 ± 0.9**	**↓ 40 ± 6**
8	29.9 ± 3.4	132.9 ± 12	22.5 ± 2.4	101.1 ± 10.3	**↓ 13.4 ± 1.6**	**↓ 49.9 ± 5**	**↓ 5.8 ± 0.7**	**↓ 29.2 ± 3.6**
9	24.3 ± 3.9	99.9 ± 17.7	17.6 ± 2.1	78.8 ± 9.6	**↓ 11.2 ± 1.3**	**↓ 40.7 ± 3.5**	**↓ 4.5 ± 0.5**	**↓ 22.8 ± 2.4**
10	17.8 ± 3.3	72.3 ± 11.6	12.5 ± 2.2	52.9 ± 10.1	**↓ 8.8 ± 1.1**	**↓ 33.8 ± 3.1**	**↓ 3 ± 0.3**	**↓ 12.3 ± 1.4**

Table 5. Summary of the morphometric analysis of microglia. Effects of different treatments on the number and length of microglial processes in the PFC. Grey and blue areas represent statistically significant changes in the number or length of microglial processes, respectively. [1]Compared with Sal-treated animals. [2]Compared with DEX-treated animals.

3.2.3. Correlation between the estrous cycle phase and anxiety/depressive-related behaviour

Wistar rat females were also tested at PND90 for two different behavioural parameters: anxiety and depressive-like behaviour (unpublished data). A vaginal smear was obtained from each female involved in these tests, to determine if the hormonal balance could affect behaviour. The characterization of the smears allowed the

correlation analysis between the behavioural profile of all females (disregard of the treatment) and the respective stages of the estrous cycle – the reproductive cycle of rodents. No correlation was found between different phases of the cycle and the anxiety or depressive-like behaviour exhibited by females (fig 15E-G), as shown by the similar dispersion of individuals with several profiles in all phases of the estrous cycle.

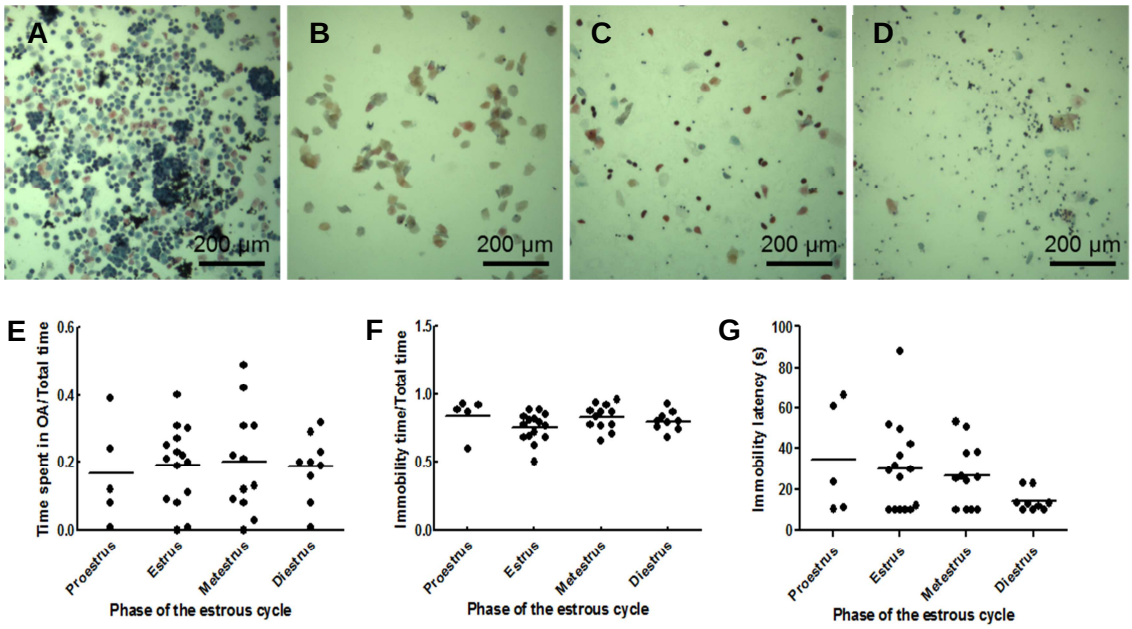

Figure 15. Correlation between the stages of the estrous cycle and anxious/depressive-like behaviour. Pregnant females were injected with DEX (1 mg/kg sc) or Sal during pregnancy (ED 18 and 19). At adulthood, animals from both groups were injected with SCH58261 (0.1 mg/kg ip) or Sal for 3 weeks before PND90. Before task behaviours at PND90 (executed and analysed in previous work), smears were obtained from female Wistar rats and stained by haematoxylin and eosin, to assess in what stage of the reproductive cycle they were at. Representative images of each of the four stages are presented: **(A)** proestrus, **(B)** estrus, **(C)** metestrus and **(D)** diestrus. **(E)** Quantification of anxiety–related behaviour was obtained through performances on the EPM (conducted and analysed previously [Caetano, 2014]) and, after classification of the correspondent smears, both parameters were correlated. The FST was used to assess depressive-like behaviour. The data were also correlated with the stage of the reproductive cycle for each animal. From this test, two parameters are assessed: **(F)** the immobility to total time ratio **(G)** and the immobility latency. Results are expressed as mean ± SEM of 5-15 animals (one-way ANOVA).

3.2.4. Impact of dexamethasone and chronic adenosine A_{2A} receptors blockade on serum corticosterone levels

CORT is the physiological GC in rodents. Secretion is more elevated during the activity period (day for humans and night for rodents), with a peak at the start of this interval (Chung et al., 2011). In rodents, peaks are similar but inversed, once they are nocturnal animals. For that reason, CORT levels were measured at two time points in all evaluated animals: 8:00 am (when lights were turned on) and 8:00 pm (lights off). Blood samples were drawn from these animals at both times of the day through

puncture of the tail vein and CORT was quantified. Comparisons were carried out between samples obtained at the same hour. i*u*DEX decreased morning levels of CORT (81.4 ± 7.9 %, p>0.05, compared with Sal-treated animals), while chronic $A_{2A}R$ blockade in adulthood decreased the evening levels (78.7 ± 4.6 %, p>0.05, compared with Sal-treated animals). Chronic SCH58261 administration at adult age in animals treated with *iu*DEX, CORT serum concentration decreased in the morning (86.8 ± 2.7, p>0.05, compared with Sal-treated animals) and in the evening (73.6 ± 8.3, p>0.05, compared with DEX-treated animals) (fig. 16).

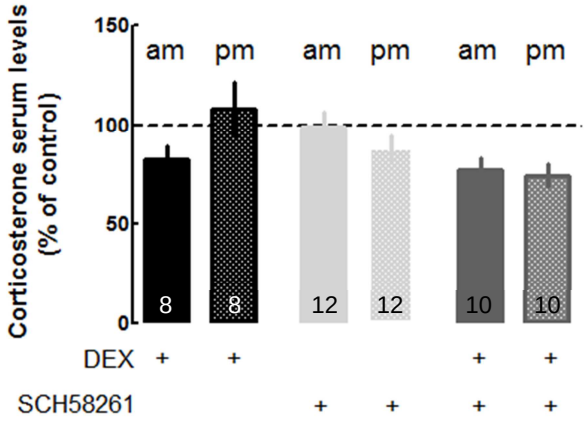

Figure 16. Effect of dexamethasone and/or adenosine A_{2A} receptors blockade on the serum CORT levels. Pregnant females were injected with DEX (1 mg/kg sc) or Sal during pregnancy (ED 18 and 19). At adulthood, animals from both groups were injected with SCH58261 (0.1 mg/kg ip) or Sal for 3 weeks before PND90. One day before task behaviours taking place at PND90, blood was collected from animals by tail venipuncture. The collected samples were then quantified. Results are expressed as mean ± standard error of the mean (SEM) of 8-12 animals (one-way ANOVA).

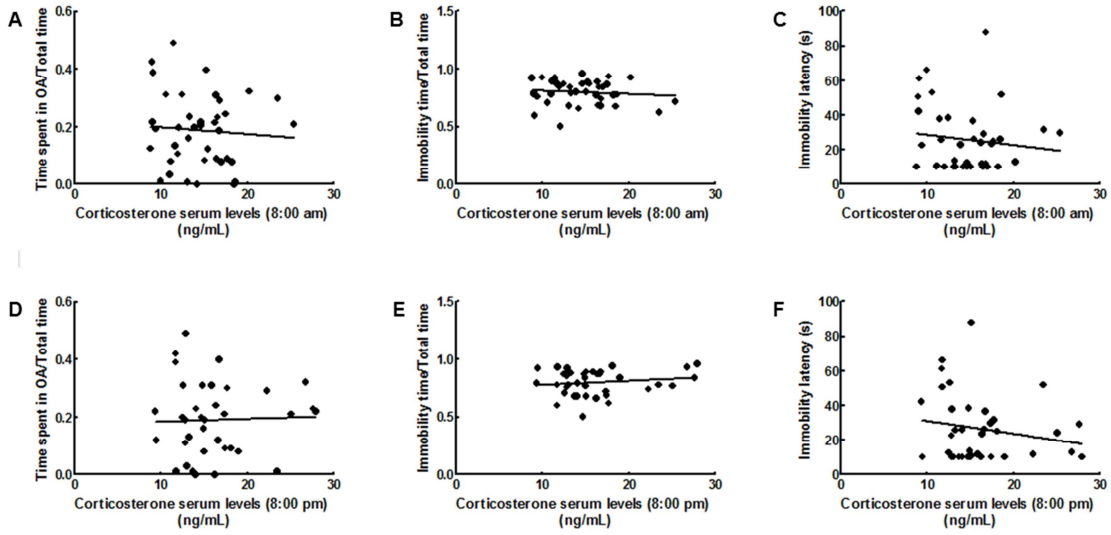

Figure 17. Correlation between serum CORT levels and behavioural performances. Pregnant females were injected with DEX (1 mg/kg sc) or Sal during pregnancy (ED 18 and 19). At adulthood, animals from both groups were injected with SCH58261 (0.1 mg/kg ip) or Sal for 3 weeks before PND90. One day before task behaviours taking place

at PND90, blood was collected from animals by tail venipuncture at 8:00 am and 8:00 pm. The collected samples were then quantified and correlated with results from the behavioural tests, namely the **(A, D)** EPM (more time in the OA reflects increased levels of anxious-like behaviour) and the (**B, C, E, F**) FST (more immobility time indicates more depressive-related behaviour). Results are expressed as mean ± standard error of the mean (SEM) of 8-12 animals (one-way ANOVA). OA, open arm.

Pearson correlation between CORT levels and the two behavioural tests (for anxiety- and depressive-related behaviour) was also performed as well (fig. 17).

By calculating Pearson (P) correlation coefficient, a value ranging from -1 to 1 is found. If P=1, the two variables are positively correlated (does not imply causation); if P=-1 the variables are negatively correlated. On the other hand, P=0 means that there is no correlation between CORT levels and the respective behavioural performances. The P value for all correlations was close to 0 (table 6).

	CORT levels (8:00 am)	CORT levels (8:00 pm)
Time spent in OA/Total time	- 0.07 (p=0.7)	- 0.04 (p=0.8)
Immobility time/Total time	- 0.11 (p=0.5)	- 0.16 (p=0.4)
Immobility latency (s)	- 0.12 (p=0.5)	- 0.18 (p=0.3)

Table 6. Summary of the Pearson correlation values (P) and respective statistical analysis (p).

Once P values are, globally, close to 0, these results imply no correlation between both variables, whatever the test is – anxious- or depressive-like behaviour.

CHAPTER 4

DISCUSSION

Microglia are not only associated with the maintenance of basal conditions in the brain, assuming a defining role during brain development, contributing in a large extent to elimination and formation of synapses (Paolicelli et al., 2011; Lim et al., 2013; Parkhurst et al., 2013; Cristóvão et al., 2014). This last functional role was one of the reasons why microglia was considered in the present work as a candidate for mediating the deleterious effects of prenatal exposure to DEX, a synthetic GC, in the brain circuitry of adults, once microglia expresses functional GR (Sierra et al., 2008). These effects include neuronal death and dendritic atrophy (Cerqueira et al., 2005; Cerqueira et al., 2007).

The main findings of this work are that microglial morphology, besides being directly altered by DEX, an effect prevented by previous blockade of $A_{2A}R$ *in vitro*, also reacts to this drug *in vivo*. *iu*DEX decreases the number and length of processes, a response exacerbated by blockade of $A_{2A}R$ at adult age. GR and $A_{2A}R$ densities are also changed throughout the brain in a region-dependent manner by the same treatments. CORT serum levels were also diminished in animals treated with *iu*DEX or/and $A_{2A}R$ antagonist later (SCH58261) in life.

Research preceding the presented results show that microglia is significantly altered in the PFC of animals aged 1, 7 and 90 days, which translates into fewer and shorter processes (Caetano, 2014). However, in order to assess if microglial cells were directly affected by DEX (and not only indirectly by alterations in the brain environment), *in vitro* studies were conducted.

Morphological categorization of microglia *in vitro* (N9 cell line) is a rather complex process. The first reason is that cells are quite different from those encountered on the brain parenchyma, being much less ramified. The culture of microglial cells is a process that, without any additional treatment, renders cells more amoeboid. Given that microglia work as sensors in the CNS, such a drastic difference in their growth environment has an immediate effect on their morphology. Moreover, even though cultured microglia are not as ramified, the phenotypes that exist are so variable that it becomes hard to set rigid criteria. Only two groups were chosen to carry out the analysis, once this was the more realistic and revealing form of assessing microglia morphology: amoeboid or ramified. The measure for the impact of pharmacological treatment was the variation in the ratio of cells belonging to either group.

In non-treated cells, microglia are mostly amoeboid due to the basal activation that occurs in culture. When DEX is added, the percentage of ramified cells in the culture increases, confirming that microglia are directly affected by DEX. At first sight, these *in*

vitro experiments appear to enter in conflict with previous findings, once *iu*DEX has been shown to decrease the number and length of microglial processes *in vivo* (Caetano, 2014). However, the brain environment is more complex than a culture flask, given that its constitution also includes neurons and other types of glial cells (oligodendrocytes, for example). Therefore, a correct analysis has to take into account the interactions that become subtracted *in vitro*.

The addition of SCH58261 did not lead to a significant difference in the distribution of phenotypes in the microglial population *in vitro*. The lack of differences induced by SCH58261 was expected, as this $A_{2A}R$ inhibitor usually plays a role *in vitro* not by itself, but in response to other stimuli, such as LPS or glutamate (Gomes et al., 2013; George et al., 2015). Of note, pre-incubation with SCH58261 before DEX tended to prevent the morphological changes induced by DEX. However, further studies are needed to confirm these preliminary data.

In the *in vivo* experiments, in order to assess the impact of the mentioned drugs, it became crucial to study the ontogeny of the respective receptors: GR and $A_{2A}R$. Two of the time points considered in this study have already been analysed (Caetano, 2014); the present work focused on analysing differences in their density in the brain in adulthood. Exposure to *iu*DEX with or without chronic administration of SCH58261 in adulthood, as well as the chronic administration of SCH58261 without *iu*DEX, altered the density of $A_{2A}R$ and GR differently according to the brain region analysed. This panel of quantifications provides important information: first, the striatum appeared to be very sensitive to DEX and SCH58261 administration (together and separately). Second, combining the results for the PFC (region of interest) with others from previous work (Caetano, 2014), it becomes noticeable that DEX had propensity to decrease $A_{2A}R$ levels over the lifespan of the animal. In parallel, it initially increased those of GR, bringing them back to control levels in adulthood. These observations reinforce the mutual control of both systems and the hypothesis that the *iu*DEX-induced microglial alterations are mediated by $A_{2A}R$, a possibility to be further explored.

The main purpose of the present thesis was centered on the morphometric analysis of microglial processes using the Neurolucida software. After obtaining a three-dimensional image of microglia cells, this software allows for a detailed reproduction of the cell structure through manual drawing of ramifications. Because every branch is reproduced in the plane where it is found in the biological preparation, the result of this methodology is a digital version of the original cell, also three-dimensional, accompanied by morphometric data. Even though the software offers the possibility for

automatic reconstruction, all tasks were performed using manual reconstruction, to avoid a greater margin of error (verified by pilot studies).

This particular form of structural replication (manual) has a demand related to criteria. These must be very well established and maintained throughout the entire process, a rule for any laboratory technique, in order to avoid interpersonal variations in the analysis protocol. Having that in mind, a validation of previous observations was conducted, comparing the data from non-treated animals with animals exposed to *iu*DEX (Caetano, 2014). The results concerning the number of processes belonging to each order agreed with prior work: DEX significantly decreased the number of processes in order 6 (Caetano, 2014). Despite the statistical significance of the decrease in order 6, the number of processes is globally diminished in animals treated with *iu*DEX. The degree of ramification near the cell body is not altered – both conditions are quite similar. However, as the order increases, so does the difference between the respective numbers of processes, a pattern that is in line with previous observations (Caetano, 2014).

In terms of process length, it was globally decreased by DEX. However, only in order 6 DEX significantly shortened the cell processes. Other reports have stated that stress induces the increase of the length of processes in the PFC (Hinwood et al, 2012). This discrepancy may be due to differences in the age of the animals (even though stress is the tested condition, instead of *iu*DEX), once the aforementioned study consists of protocols taking place during adulthood. This hypothesis is strengthened by another report that claims that DEX can diminish the perimeter of microglia isolated from the forebrain of newborn rats (Tanaka et al., 1997). Importantly, this decrease in the length and number of processes is already at PND 1 and PND 7. These observations are quite relevant once they show that the administration of DEX in a critical point of neurodevelopment is responsible for alterations in microglia ramification that persist until adulthood.

The second set of results within the morphometric analysis, regarding the administration of SCH58261, showed that the blockade of the $A_{2A}R$ is not able to reverse DEX-induced morphologic alterations. Several times over the years, $A_{2A}R$ blockade granted neuroprotection in more than one animal model of pathology (Chen et al., 2001; Yu, et al., 2008; Canas et al., 2009). This shielding characteristic allied to findings that render $A_{2A}R$ fundamental for the dynamics of microglial processes were the basis for the work hypothesis centered on the reversal of *iu*DEX-induced morphologic alterations in microglia and anxiety-related phenotype through the

blockade of $A_{2A}R$. The present results showed that the administration of SCH58261 not only reduced the length of processes in almost every order, but also decreased the number of ramifications attributed to orders 4 to 10, with no significant effect for the remaining three. Enlightening studies have clarified in the past few years the mechanistics of $A_{2A}R$ involvement in branch movement (Orr et al., 2009; Gyoneva et al., 2014). What is known is that microglia, when unperturbed, can be chemoattracted to a site of injury by sensing ATP, responding afterwards by extending the respective processes. However, when microglia presents itself in a state classified as activated, ATP exposure leads to process retraction (Orr et al., 2009; Gyoneva et al., 2014). Of note, in activated microglia there is downregulation of the ATP receptor $P2Y_{12}$ and upregulation of $A_{2A}R$ (Wittendorp et al., 2004; Haynes et al., 2006). What is considered an activation profile in these studies consists of the phenotype triggered by LPS exposure, namely increased levels of anti-inflammatory cytokines such as IL-1β and TNF-α. In this particular case, (1) SCH58261 administration tended to decrease $A_{2A}R$ levels in the PFC and (2) DEX is an anti-inflammatory glucocorticoid. This particular context is not contemplated in the aforementioned studies. This information suggests that $A_{2A}R$ have a fundamental (and not redundant) role on microglial process formation during neurodevelopment and in a non-pathological scenario.

The administration of SCH58261 at adulthood was not able to reverse the phenotypic changes induced by *iu*DEX. Instead, these became exacerbated when compared to the administration of DEX or SCH58261 separately. Still, these results are very important for two different reasons. First, it was verified that DEX created morphologic reshaping of microglia, decreasing the number and length of processes. Secondly, they also open room for discussion regarding a physiological and irreplaceable new role for $A_{2A}R$ in the definition of microglia morphology during neurodevelopment.

All the animal experiments that gave rise to the present thesis were conducted on female Wistar rats. It is important to evaluate the effects of the glucocorticoid DEX on both genders separately for two reasons. First, in the clinical context, women are more prone to stress-related mental disorders than men (Linzer et al., 1996; Van de Velde et al., 2010). Secondly, this gender has a very important factor to take into account: the reproductive cycle (estrous cycle in rodents). Once the HPA axis is influenced by the levels of gonadal hormones (Kitay et al., 1963; Viau et al., 2001; Handa et al., 2013), several studies have been conducted trying to determine their correlation in a stressful situation in both genders. Females, but not males, have been shown to display behavioural deficits and synaptic alterations in the hippocampus after chronic restraint stress in adulthood (Rico et al., 2015). On the other hand, a study where DEX was

administered prenatally asserts that the dopaminergic populations of males are more affected by the treatment than females (McArthur et al., 2005). The type of stressor is determinant on the gender-specific differences observed in the activity of the HPA axis (Babb et al., 2013). However, many studies have confirmed that there is a relationship between the HPA axis and the estrous cycle, whether they refer to the sensitivity of the axis according to the stage of the cycle (Viau et al., 1991) or the impact that stress has in the length of those same stages (Mourlon et al., 2011). Taking into consideration all of these factors, it would be negligent to conduct a study about GC in female rats exclusively without checking for the estrous cycle in each individual and, importantly, correlating this with their behavioural phenotypes. The goal of this particular analysis was to see if there was a particular moment during the reproductive cycle of the rat that rendered it more (or less) prone to a particular profile. Our observations revealed that, in this particular model, there was no correlation between any particular stage of the estrous cycle and the anxiety- or depressive-associated behaviour (not accounting for the treatment). Data from different treatments were not processed separately because there were not sufficient individuals per stage in all treatments to obtain solid conclusions, even though that particular analysis would be very useful as well.

Studies in the field have revealed that alterations in HPA axis activity in embryonic life may alter the basal levels of CORT during adulthood. The gender is a factor in this alteration: one study using antenatal DEX has shown that this leads to increased levels of CORT in females, whereas males have decreased blood CORT (Liu et al., 2001) Regimen of administration is also important once a different model of prenatal DEX gave rise to increased CORT levels in males (Levitt al al., 1996). In the clinical practice, anxiety (also observed in animals exposed to *iu*DEX) is usually characterized by increased levels of cortisol – chronical hypercortisolemia (Bhagwagar et al., 2005). However, by unclear reasons, there are also pathologically anxious patients that present with the opposite phenotype: hypocortisolemia (Bremmer et al., 2007; Penninx et al., 2007). What becomes evident is that there is still an incomplete understanding of the regulation of cortisol/CORT levels by different HPA axis-related pathologies. Therefore, the data here presented is informative for a very specific situation and, for that reason, must be very sceptically correlated with other scenarios involving GC. Nevertheless, regarding the animal model used to obtain the results here presented, previous CORT measurements have only been able to detect a slight tendency to increase in animals treated with DEX (Oliveira et al., 2006). Decreases in CORT serum levels were observed in the present thesis: in the morning levels for DEX exposure, in evening levels upon SCH58261 administration and in both time points for treatment

with SCH58261 after previous DEX injection *in utero*. These results are interesting from a dual perspective: first, they may suggest exhaustion of the HPA axis by overstimulation, a concept considered by others (Vreeburg et al., 2013). On the other hand, it is equally interesting to observe a parallel, however limited, to the morphometric analysis of microglia: even though DEX and SCH58261 treatments, when applied in separate, have a different outcome, their conjugation seems to result in an accumulation of those effects, attesting for a transversal consistency of effects.

No correlation was observed between CORT levels and behavioural outcomes. Importantly, correlation tests do not enable conclusions related to causational effects, meaning that even though there is no obvious correlation between the values, no additional conclusion may be inferred on how they influence each other.

CHAPTER 5

CONCLUSIONS AND FUTURE DIRECTIONS

In this study, the effect of *iu*DEX on microglial morphology during adulthood was confirmed to exist, in addition to findings that this cell population is already altered at PND 1 and PND 7 (fewer and shorter processes, Caetano, 2014). This effect consists of a decrease in both the number and length of microglial processes. Blockade of $A_{2A}R$ (SCH58261) in adult age without any additional treatment also altered microglial morphology with an effect on the branch structure of almost every order – fewer and shorter processes. By blocking $A_{2A}R$ in adulthood after previous prenatal treatment with DEX, the effect of SCH58261 was exacerbated. In parallel, the analysis of both receptors of interest at PND90 in the PFC (enriched in GR and in charge of mood and HPA axis control) was also conducted, attesting that both of them were altered at this stage. Putting the collected data together with previous ones, a pattern seems to arise where they evolve ontogenically in opposite directions: while GR were increased in early stages of life and then resumed to control, $A_{2A}R$ in the first days of life were found at control levels and then, in adulthood, presented with a tendency to decrease. Once the entire study was conducted in females, their performances at behavioural tests (for anxiety and depressive-like behaviour, not analysed here) were correlated with their estrous cycle at the time – no relation between both was detected. Basal levels of CORT were not significantly different among treatments, despite a tendency to decrease with DEX, SCH58261 or both.

Despite these findings, several lines of work are still open. First, it is important to understand how important the microglia role is in the process of synaptic impairment triggered by DEX. For this, a possible approach would be depleting microglia (through clodronate liposomes) in brain slices and posteriorly add DEX. After that, an analysis of the neuronal structure, particularized at neuronal sites, and quantification of immature synapses would allow discriminating the influence of microglia on the DEX-induced synaptic rearrangement.

It would also be of interest to repeat the analyses performed in the present thesis, as well as the already mentioned assessment of immature synapses, in animals subjected to a chronic stress protocol, once liability to depression is a trait in this animal model and in the clinical practice.

An interesting path to pursuit as well would be the role of $A_{2A}R$ in maintaining proper microglial structure in the absence of an insult in adult age. The blockade of these receptors has been considered neuroprotective for a myriad of pathological situations, a paradigm that does not fit this particular model. However, the present observations

imply that their presence is clearly not redundant, indicating that $A_{2A}R$ may be approached from a different point of view in particular contexts.

Finally, once the blockade of $A_{2A}R$ was not able to reverse microglial morphologic rearrangements induced by DEX, new options may be considered for this purpose, namely antidepressants and mood stabilizers, such as lithium. Lithium is frequently prescribed in the clinic, mostly to treat bipolar disorder. The precise mechanism is unknown, but given that the adult phenotype of *iu*DEX-treated individuals consists of increased levels of anxiety and liability to depression, an insight on the applicability of this compound to this particular model could be of interest.

CHAPTER 6

REFERENCES

Adair TH. Growth regulation of the vascular system: an emerging role for adenosine. Am J Physiol Regul Integr Comp Physiol. 2005;289(2):R283-R96.

Babb JA, Masini CV, Day HE, Campeau S. Stressor-specific effects of sex on HPA axis hormones and activation of stress-related neurocircuitry. Stress. 2013;16(6):664-77.

Baldwin SA, Mackey JR, Cass CE, Young JD. Nucleoside transporters: molecular biology and implications for therapeutic development. Mol Med Today. 1999;5(5):216-24.

Banasr M, Duman RS. Glial loss in the prefrontal cortex is sufficient to induce depressive-like behaviors. Biol Psychiatry. 2008;64(10):863-70.

Batalha VL, Pego JM, Fontinha BM, Costenla AR, Valadas JS, Baqi Y, et al. Adenosine A_{2A} receptor blockade reverts hippocampal stress-induced deficits and restores corticosterone circadian oscillation. Mol Psychiatry. 2013;18(3):320-31.

Bhagwagar Z, Hafizi S, Cowen PJ. Increased salivary cortisol after waking in depression. Psychopharmacology (Berl). 2005;182(1):54-7.

Bremmer MA, Deeg DJ, Beekman AT, Penninx BW, Lips P, Hoogendijk WJ. Major depression in late life is associated with both hypo- and hypercortisolemia. Biol Psychiatry. 2007;62(5):479-86.

Broch OJ, Ueland PM. Regional and subcellular distribution of S-adenosylhomocysteine hydrolase in the adult rat brain. J Neurochem. 1980;35(2):484-8.

Brownfoot FC, Gagliardi DI, Bain E, Middleton P, Crowther CA. Different corticosteroids and regimens for accelerating fetal lung maturation for women at risk of preterm birth. Cochrane Database Syst Rev. 2013;8:CD006764.

Brundege JM, Diao L, Proctor WR, Dunwiddie TV. The role of cyclic AMP as a precursor of extracellular adenosine in the rat hippocampus. Neuropharmacology. 1997;36(9):1201-10.

Byers SL, Wiles MV, Dunn SL, Taft RA. Mouse estrous cycle identification tool and images. PLoS One. 2012;7(4):e35538.

Caetano, Liliana Ricardina Oliveira. Purinergic involvement in microglial responses to

immunomodulation during neurodevelopment. 2014. 95 f. Dissertação (Mestrado em Bioquímica). Universidade de Coimbra, Coimbra.

Caligioni CS. Assessing reproductive status/stages in mice. Curr Protoc Neurosci. 2009;Appendix 4:Appendix 4I.

Canas PM, Porciuncula LO, Cunha GM, Silva CG, Machado NJ, Oliveira JM, et al. Adenosine A_{2A} receptor blockade prevents synaptotoxicity and memory dysfunction caused by beta-amyloid peptides via p38 mitogen-activated protein kinase pathway. J Neurosci. 2009;29(47):14741-51.

Cerqueira JJ, Pego JM, Taipa R, Bessa JM, Almeida OF, Sousa N. Morphological correlates of corticosteroid-induced changes in prefrontal cortex-dependent behaviors. J Neurosci. 2005;25(34):7792-800.

Cerqueira JJ, Taipa R, Uylings HB, Almeida OF, Sousa N. Specific configuration of dendritic degeneration in pyramidal neurons of the medial prefrontal cortex induced by differing corticosteroid regimens. Cereb Cortex. 2007;17(9):1998-2006.

Chen JF, Xu K, Petzer JP, Staal R, Xu YH, Beilstein M, et al. Neuroprotection by caffeine and A_{2A} adenosine receptor inactivation in a model of Parkinson's disease. J Neurosci. 2001;21(10):RC143.

Chung S, Son GH, Kim K. Circadian rhythm of adrenal glucocorticoid: its regulation and clinical implications. Biochim Biophys Acta. 2011;1812(5):581-91.

Cooke RR, McIntosh JE, Murray-McIntosh RP. Effect of cortisol on percentage of non-sex-hormone-bound steroid: implications for distribution of steroids on binding proteins in serum. Clin Chem. 1996;42(2):249-54.

Cristóvão G, Pinto MJ, Cunha RA, Almeida RD, Gomes CA. Activation of microglia bolsters synapse formation. Front Cell Neurosci. 2014;8:153.

Cunha GM, Canas PM, Oliveira CR, Cunha RA. Increased density and synapto-protective effect of adenosine A_{2A} receptors upon sub-chronic restraint stress. Neuroscience. 2006;141(4):1775-81.

Cunha RA. Adenosine as a neuromodulator and as a homeostatic regulator in the nervous system: different roles, different sources and different receptors. Neurochem Int. 2001;38(2):107-25.

Cunningham CL, Martinez-Cerdeno V, Noctor SC. Microglia regulate the number of neural precursor cells in the developing cerebral cortex. J Neurosci. 2013;33(10):4216-33.

Dai SS, Zhou YG, Li W, An JH, Li P, Yang N, et al. Local glutamate level dictates adenosine A2A receptor regulation of neuroinflammation and traumatic brain injury. J Neurosci. 2010;30(16):5802-10.

Dalmau I, Finsen B, Zimmer J, Gonzalez B, Castellano B. Development of microglia in the postnatal rat hippocampus. Hippocampus. 1998;8(5):458-74.

Dalmau I, Vela JM, Gonzalez B, Finsen B, Castellano B. Dynamics of microglia in the developing rat brain. J Comp Neurol. 2003;458(2):144-57.

Davalos D, Grutzendler J, Yang G, Kim JV, Zuo Y, Jung S, et al. ATP mediates rapid microglial response to local brain injury in vivo. Nat Neurosci. 2005;8(6):752-8.

De Kloet ER, Van Acker SA, Sibug RM, Oitzl MS, Meijer OC, Rahmouni K, et al. Brain mineralocorticoid receptors and centrally regulated functions. Kidney Int. 2000;57(4):1329-36.

De Kloet ER, Vreugdenhil E, Oitzl MS, Joels M. Brain corticosteroid receptor balance in health and disease. Endocr Rev. 1998;19(3):269-301.

Dias RB, Rombo DM, Ribeiro JA, Henley JM, Sebastiao AM. Adenosine: setting the stage for plasticity. Trends Neurosci. 2013;36(4):248-57.

Dias RB, Rombo DM, Ribeiro JA, Henley JM, Sebastiao AM. Adenosine: setting the stage for plasticity. Trends Neurosci. 2013;36(4):248-57.

Diaz Heijtz R, Fuchs E, Feldon J, Pryce CR, Forssberg H. Effects of antenatal dexamethasone treatment on glucocorticoid receptor and calcyon gene expression in the prefrontal cortex of neonatal and adult common marmoset monkeys. Behav Brain Funct. 2010;6:18.

Dixon AK, Gubitz AK, Sirinathsinghji DJ, Richardson PJ, Freeman TC. Tissue distribution of adenosine receptor mRNAs in the rat. Br J Pharmacol. 1996;118(6):1461-8.

Dobbing J, Sands J. Comparative aspects of the brain growth spurt. Early Hum Dev. 1979;3(1):79-83. Drozdowicz LB, Bostwick JM. Psychiatric adverse effects of pediatric corticosteroid use. Mayo Clin Proc. 2014;89(6):817-34.

Drozdowicz LB, Bostwick JM. Psychiatric adverse effects of pediatric corticosteroid use. Mayo Clin Proc. 2014;89(6):817-34.

El Yacoubi M, Ledent C, Parmentier M, Bertorelli R, Ongini E, Costentin J, et al. Adenosine A_{2A} receptor antagonists are potential antidepressants: evidence based on pharmacology and A_{2A} receptor knockout mice. Br J Pharmacol. 2001;134(1):68-77.

Elkabes S, Peng L, Black IB. Lipopolysaccharide differentially regulates microglial trk receptor and neurotrophin expression. J Neurosci Res. 1998;54(1):117-22.

Fiebich BL, Biber K, Lieb K, van Calker D, Berger M, Bauer J, et al. Cyclooxygenase-2 expression in rat microglia is induced by adenosine A2a-receptors. Glia. 1996;18(2):152-60.

Frade JM, Barde YA. Microglia-derived nerve growth factor causes cell death in the developing retina. Neuron. 1998;20(1):35-41.

Frank MG, Baratta MV, Sprunger DB, Watkins LR, Maier SF. Microglia serve as a neuroimmune substrate for stress-induced potentiation of CNS pro-inflammatory cytokine responses. Brain Behav Immun. 2007;21(1):47-59.

Frank MG, Miguel ZD, Watkins LR, Maier SF. Prior exposure to glucocorticoids sensitizes the neuroinflammatory and peripheral inflammatory responses to E. coli lipopolysaccharide. Brain Behav Immun. 2010;24(1):19-30.

Fredholm BB, AP IJ, Jacobson KA, Klotz KN, Linden J. International Union of Pharmacology. XXV. Nomenclature and classification of adenosine receptors. Pharmacol Rev. 2001;53(4):527-52.

Fredholm BB, Chen JF, Cunha RA, Svenningsson P, Vaugeois JM. Adenosine and brain function. Int Rev Neurobiol. 2005;63:191-270.

George J, Goncalves FQ, Cristovao G, Rodrigues L, Meyer Fernandes JR, Goncalves T, et al. Different danger signals differently impact on microglial proliferation through alterations of ATP release and extracellular metabolism. Glia. 2015.

Ginhoux F, Greter M, Leboeuf M, Nandi S, See P, Gokhan S, et al. Fate mapping analysis reveals that adult microglia derive from primitive macrophages. Science. 2010;330(6005):841-5.

Ginhoux F, Lim S, Hoeffel G, Low D, Huber T. Origin and differentiation of microglia. Front Cell Neurosci. 2013;7:45.

Gomes C, Ferreira R, George J, Sanches R, Rodrigues DI, Goncalves N, et al. Activation of microglial cells triggers a release of brain-derived neurotrophic factor (BDNF) inducing their proliferation in an adenosine A_{2A} receptor-dependent manner: A_{2A} receptor blockade prevents BDNF release and proliferation of microglia. J Neuroinflammation. 2013;10:16.

Gomes CV, Kaster MP, Tome AR, Agostinho PM, Cunha RA. Adenosine receptors and brain diseases: neuroprotection and neurodegeneration. Biochim Biophys Acta. 2011;1808(5):1380-99.

Graeber MB. Changing face of microglia. Science. 2010;330(6005):783-8.

Gyoneva S, Shapiro L, Lazo C, Garnier-Amblard E, Smith Y, Miller GW, et al. Adenosine A_{2A} receptor antagonism reverses inflammation-induced impairment of microglial process extension in a model of Parkinson's disease. Neurobiol Dis. 2014;67:191-202.

Handa RJ, Weiser MJ. Gonadal steroid hormones and the hypothalamo-pituitary-adrenal axis. Front Neuroendocrinol. 2014;35(2):197-220.

Haynes SE, Hollopeter G, Yang G, Kurpius D, Dailey ME, Gan WB, et al. The P2Y12 receptor regulates microglial activation by extracellular nucleotides. Nat Neurosci. 2006;9(12):1512-9.

Heese K, Fiebich BL, Bauer J, Otten U. Nerve growth factor (NGF) expression in rat microglia is induced by adenosine A_{2A}-receptors. Neurosci Lett. 1997;231(2):83-6.

Herman JP, Cullinan WE. Neurocircuitry of stress: central control of the hypothalamo-pituitary-adrenocortical axis. Trends Neurosci. 1997;20(2):78-84.

Herman JP, Ostrander MM, Mueller NK, Figueiredo H. Limbic system mechanisms of stress regulation: hypothalamo-pituitary-adrenocortical axis. Prog Neuropsychopharmacol Biol Psychiatry. 2005;29(8):1201-13.

Hettinger BD, Lee A, Linden J, Rosin DL. Ultrastructural localization of adenosine A_{2A} receptors suggests multiple cellular sites for modulation of GABAergic neurons in rat striatum. J Comp Neurol. 2001;431(3):331-46.

Hinwood M, Tynan RJ, Charnley JL, Beynon SB, Day TA, Walker FR. Chronic stress induced remodeling of the prefrontal cortex: structural re-organization of microglia and the inhibitory effect of minocycline. Cereb Cortex. 2013;23(8):1784-97.

Huo Y, Rangarajan P, Ling EA, Dheen ST. Dexamethasone inhibits the Nox-dependent ROS production via suppression of MKP-1-dependent MAPK pathways in activated microglia. BMC Neurosci. 2011;12:49.

immunomodulation during neurodevelopment. 2003. 95 p. Dissertation (Master's degree in Biochemistry). Faculty of Sciences and Technology, University of Coimbra, Portugal.

Ito D, Imai Y, Ohsawa K, Nakajima K, Fukuuchi Y, Kohsaka S. Microglia-specific localisation of a novel calcium binding protein, Iba1. Brain Res Mol Brain Res. 1998;57(1):1-9.

Jin X, Shepherd RK, Duling BR, Linden J. Inosine binds to A3 adenosine receptors and stimulates mast cell degranulation. J Clin Invest. 1997;100(11):2849-57.

Kaster MP, Machado NJ, Silva HB, Nunes A, Ardais AP, Santana M, et al. Caffeine acts through neuronal adenosine A2A receptors to prevent mood and memory dysfunction triggered by chronic stress. Proc Natl Acad Sci U S A. 2015.

Kettenmann H, Hanisch UK, Noda M, Verkhratsky A. Physiology of microglia. Physiol Rev. 2011;91(2):461-553.

Kettenmann H, Kirchhoff F, Verkhratsky A. Microglia: new roles for the synaptic stripper. Neuron. 2013;77(1):10-8.

Kitay JI. Pituitary-Adrenal Function in the Rat after Gonadectomy and Gonadal Hormone Replacement. Endocrinology. 1963;73:253-60.

Kull B, Svenningsson P, Fredholm BB. Adenosine A_{2A} receptors are colocalized with and activate g(olf) in rat striatum. Mol Pharmacol. 2000;58(4):771-7.

Kust BM, Biber K, van Calker D, Gebicke-Haerter PJ. Regulation of K+ channel mRNA expression by stimulation of adenosine A_{2A}-receptors in cultured rat microglia. Glia. 1999;25(2):120-30.

Latini S, Pedata F. Adenosine in the central nervous system: release mechanisms and extracellular concentrations. J Neurochem. 2001;79(3):463-84.

Leão P, Sousa JC, Oliveira M, Silva R, Almeida OF, Sousa N. Programming effects of antenatal dexamethasone in the developing mesolimbic pathways. Synapse. 2007;61(1):40-9.

Levitt NS, Lindsay RS, Holmes MC, Seckl JR. Dexamethasone in the last week of pregnancy attenuates hippocampal glucocorticoid receptor gene expression and elevates blood pressure in the adult offspring in the rat. Neuroendocrinology. 1996;64(6):412-8.

Lewis DA, Smith RE. Steroid-induced psychiatric syndromes. A report of 14 cases and a review of the literature. J Affect Disord. 1983;5(4):319-32.

Li P, Rial D, Canas PM, Yoo JH, Li W, Zhou X, et al. Optogenetic activation of intracellular adenosine A receptor signaling in the hippocampus is sufficient to trigger CREB phosphorylation and impair memory. Mol Psychiatry. 2015.

Lim SH, Park E, You B, Jung Y, Park AR, Park SG, et al. Neuronal synapse formation induced by microglia and interleukin 10. PLoS One. 2013;8(11):e81218.

Linzer M, Spitzer R, Kroenke K, Williams JB, Hahn S, Brody D, et al. Gender, quality of life, and mental disorders in primary care: results from the PRIME-MD 1000 study. Am J Med. 1996;101(5):526-33.

Liu L, Li A, Matthews SG. Maternal glucocorticoid treatment programs HPA regulation in adult offspring: sex-specific effects. Am J Physiol Endocrinol Metab. 2001;280(5):E729-39.

Lloyd HG, Fredholm BB. Involvement of adenosine deaminase and adenosine kinase in regulating extracellular adenosine concentration in rat hippocampal slices. Neurochem Int. 1995;26(4):387-95.

Lu NZ, Wardell SE, Burnstein KL, Defranco D, Fuller PJ, Giguere V, et al. International Union of Pharmacology. LXV. The pharmacology and classification of the nuclear receptor superfamily: glucocorticoid, mineralocorticoid, progesterone, and androgen receptors. Pharmacol Rev. 2006;58(4):782-97.

Madrigal JL, Moro MA, Lizasoain I, Lorenzo P, Fernandez AP, Rodrigo J, et al. Induction of cyclooxygenase-2 accounts for restraint stress-induced oxidative status in rat brain. Neuropsychopharmacology. 2003;28(9):1579-88.

Magnus T, Chan A, Linker RA, Toyka KV, Gold R. Astrocytes are less efficient in the removal of apoptotic lymphocytes than microglia cells: implications for the role of glial cells in the inflamed central nervous system. J Neuropathol Exp Neurol. 2002;61(9):760-6.

Marangos PJ, Patel J, Stivers J. Ontogeny of adenosine binding sites in rat forebrain and cerebellum. J Neurochem. 1982;39(1):267-70.

Marcondes FK, Bianchi FJ, Tanno AP. Determination of the estrous cycle phases of rats: some helpful considerations. Braz J Biol. 2002;62(4A):609-14.

Marshall PN. Papanicolaou staining - a review. Microsc Acta. 1983;87(3):233-43.

McArthur S, McHale E, Dalley JW, Buckingham JC, Gillies GE. Altered mesencephalic dopaminergic populations in adulthood as a consequence of brief perinatal glucocorticoid exposure. J Neuroendocrinol. 2005;17(8):475-82.

Meijer OC, de Lange EC, Breimer DD, de Boer AG, Workel JO, de Kloet ER. Penetration of dexamethasone into brain glucocorticoid targets is enhanced in mdr1A P-glycoprotein knockout mice. Endocrinology. 1998;139(4):1789-93.

Michaud JP, Rivest S. Anti-inflammatory signaling in microglia exacerbates Alzheimer's disease-related pathology. Neuron. 2015;85(3):450-2.

Mourlon V, Naudon L, Giros B, Crumeyrolle-Arias M, Dauge V. Early stress leads to effects on estrous cycle and differential responses to stress. Physiol Behav. 2011;102(3-4):304-10.

Munhoz CD, Lepsch LB, Kawamoto EM, Malta MB, Lima Lde S, Avellar MC, et al. Chronic unpredictable stress exacerbates lipopolysaccharide-induced activation of nuclear factor-kappaB in the frontal cortex and hippocampus via glucocorticoid secretion. J Neurosci. 2006;26(14):3813-20.

Nagano M, Ozawa H, Suzuki H. Prenatal dexamethasone exposure affects anxiety-like behaviour and neuroendocrine systems in an age-dependent manner. Neurosci Res. 2008;60(4):364-71.

Nair A, Bonneau RH. Stress-induced elevation of glucocorticoids increases microglia proliferation through NMDA receptor activation. J Neuroimmunol. 2006;171(1-2):72-85.

Newby AC. Adenosine: origin and clinical roles. Adv Exp Med Biol. 1991;309A:265-70.

Newell EA, Exo JL, Verrier JD, Jackson TC, Gillespie DG, Janesko-Feldman K, et al. 2',3'-cAMP, 3'-AMP, 2'-AMP and adenosine inhibit TNF-α and CXCL10 production from activated primary murine microglia via A_{2A} receptors. Brain Res. 2015;1594:27-35.

Nimmerjahn A, Kirchhoff F, Helmchen F. Resting microglial cells are highly dynamic surveillants of brain parenchyma in vivo. Science. 2005;308(5726):1314-8.

Nishizaki T, Nagai K, Nomura T, Tada H, Kanno T, Tozaki H, et al. A new neuromodulatory pathway with a glial contribution mediated via A_{2A} adenosine receptors. Glia. 2002;39(2):133-47.

Oakley RH, Cidlowski JA. The biology of the glucocorticoid receptor: new signaling mechanisms in health and disease. J Allergy Clin Immunol. 2013;132(5):1033-44.

Oliveira JF, Dias NS, Correia M, Gama-Pereira F, Sardinha VM, Lima A, et al. Chronic stress disrupts neural coherence between cortico-limbic structures. Front Neural Circuits. 2013;7:10.

Oliveira JF, Dias NS, Correia M, Gama-Pereira F, Sardinha VM, Lima A, et al. Chronic stress disrupts neural coherence between cortico-limbic structures. Front Neural Circuits. 2013;7:10.

Oliveira M, Bessa JM, Mesquita A, Tavares H, Carvalho A, Silva R, et al. Induction of a hyperanxious state by antenatal dexamethasone: a case for less detrimental natural corticosteroids. Biol Psychiatry. 2006;59(9):844-52.

Oliveira M, Rodrigues AJ, Leao P, Cardona D, Pego JM, Sousa N. The bed nucleus of stria terminalis and the amygdala as targets of antenatal glucocorticoids: implications for fear and anxiety responses. Psychopharmacology (Berl). 2012;220(3):443-53.

Orr AG, Orr AL, Li XJ, Gross RE, Traynelis SF. Adenosine A_{2A} receptor mediates microglial process retraction. Nat Neurosci. 2009;12(7):872-8.

Paolicelli RC, Bolasco G, Pagani F, Maggi L, Scianni M, Panzanelli P, et al. Synaptic pruning by microglia is necessary for normal brain development. Science. 2011;333(6048):1456-8.

Parkhurst CN, Yang G, Ninan I, Savas JN, Yates JR, 3rd, Lafaille JJ, et al. Microglia promote learning-dependent synapse formation through brain-derived neurotrophic factor. Cell. 2013;155(7):1596-609.

Paxinos G, Watson C. The rat brain in stereotaxic coordinates. 4th edition. American Press. 1998.

Penninx BW, Beekman AT, Bandinelli S, Corsi AM, Bremmer M, Hoogendijk WJ, et al. Late-life depressive symptoms are associated with both hyperactivity and hypoactivity of the hypothalamo-pituitary-adrenal axis. Am J Geriatr Psychiatry. 2007;15(6):522-9.

Perez-Nievas BG, Garcia-Bueno B, Caso JR, Menchen L, Leza JC. Corticosterone as a marker of susceptibility to oxidative/nitrosative cerebral damage after stress exposure in rats. Psychoneuroendocrinology. 2007;32(6):703-11.

Perlman WR, Webster MJ, Herman MM, Kleinman JE, Weickert CS. Age-related differences in glucocorticoid receptor mRNA levels in the human brain. Neurobiol Aging. 2007;28(3):447-58.

Rakic P, Bourgeois JP, Eckenhoff MF, Zecevic N, Goldman-Rakic PS. Concurrent overproduction of synapses in diverse regions of the primate cerebral cortex. Science. 1986;232(4747):232-5.

Rebola N, Canas PM, Oliveira CR, Cunha RA. Different synaptic and subsynaptic localization of adenosine A_{2A} receptors in the hippocampus and striatum of the rat. Neuroscience. 2005;132(4):893-903.

Reul JM, van den Bosch FR, de Kloet ER. Relative occupation of type-I and type-II corticosteroid receptors in rat brain following stress and dexamethasone treatment: functional implications. J Endocrinol. 1987;115(3):459-67.

Ricciotti E, FitzGerald GA. Prostaglandins and inflammation. Arterioscler Thromb Vasc Biol. 2011;31(5):986-1000.

Rico AM, Mendoza AL, Duran DA, Torres Hde L, Mendoza GA, Gomez AB. The effects of chronic restraint on the morphology of ventral CA1 neurons in female Long Evans rats. Stress. 2015;18(1):67-75.

Rizzo MC, Sole D, Naspitz CK. Corticosteroids (inhaled and/or intranasal) in the treatment of respiratory allergy in children: safety vs. efficacy. Allergol Immunopathol (Madr). 2007;35(5):197-208.

Rodrigues AJ, Leao P, Pego JM, Cardona D, Carvalho MM, Oliveira M, et al. Mechanisms of initiation and reversal of drug-seeking behavior induced by prenatal exposure to glucocorticoids. Mol Psychiatry. 2012;17(12):1295-305.

Roque S, Oliveira TG, Nobrega C, Barreira-Silva P, Nunes-Alves C, Sousa N, et al. Interplay between Depressive-Like Behavior and the Immune System in an Animal Model of Prenatal Dexamethasone Administration. Front Behav Neurosci. 2011;5:4.

Rossi F, Casano AM, Henke K, Richter K, Peri F. The SLC7A7 Transporter Identifies Microglial Precursors prior to Entry into the Brain. Cell Rep. 2015;11(7):1008-17.

Sanchez MM, Young LJ, Plotsky PM, Insel TR. Distribution of corticosteroid receptors in the rhesus brain: relative absence of glucocorticoid receptors in the hippocampal formation. J Neurosci. 2000;20(12):4657-68.

Sapolsky RM, Krey LC, McEwen BS. The neuroendocrinology of stress and aging: the glucocorticoid cascade hypothesis. Endocr Rev. 1986;7(3):284-301.

Sapolsky RM. Glucocorticoids, stress, and their adverse neurological effects: relevance to aging. Exp Gerontol. 1999;34(6):721-32.

Saura J, Angulo E, Ejarque A, Casado V, Tusell JM, Moratalla R, et al. Adenosine A_{2A} receptor stimulation potentiates nitric oxide release by activated microglia. J Neurochem. 2005;95(4):919-29.

Sawchenko PE, Brown ER, Chan RK, Ericsson A, Li HY, Roland BL, et al. The paraventricular nucleus of the hypothalamus and the functional neuroanatomy of visceromotor responses to stress. Prog Brain Res. 1996;107:201-22.

Shin HK, Park SN, Hong KW. Implication of adenosine A_{2A} receptors in hypotension-induced vasodilation and cerebral blood flow autoregulation in rat pial arteries. Life Sci. 2000;67(12):1435-45.

Sierra A, Abiega O, Shahraz A, Neumann H. Janus-faced microglia: beneficial and detrimental consequences of microglial phagocytosis. Front Cell Neurosci. 2013;7:6.

Sierra A, Encinas JM, Deudero JJ, Chancey JH, Enikolopov G, Overstreet-Wadiche LS, et al. Microglia shape adult hippocampal neurogenesis through apoptosis-coupled phagocytosis. Cell Stem Cell. 2010;7(4):483-95.

Sierra A, Gottfried-Blackmore A, Milner TA, McEwen BS, Bulloch K. Steroid hormone receptor expression and function in microglia. Glia. 2008;56(6):659-74.

Silva R, Mesquita AR, Bessa J, Sousa JC, Sotiropoulos I, Leao P, et al. Lithium blocks stress-induced changes in depressive-like behavior and hippocampal cell fate: the role of glycogen-synthase-kinase-3beta. Neuroscience. 2008;152(3):656-69.

Smith MA, Thomford PJ, Mattison DR, Slikker W, Jr. Transport and metabolism of dexamethasone in the dually perfused human placenta. Reprod Toxicol. 1988;2(1):37-43.

Smith PK, Krohn RI, Hermanson GT, Mallia AK, Gartner FH, Provenzano MD, et al. Measurement of protein using bicinchoninic acid. Anal Biochem. 1985;150(1):76-85.

Smyth GP, Stapleton PP, Freeman TA, Concannon EM, Mestre JR, Duff M, et al. Glucocorticoid pretreatment induces cytokine overexpression and nuclear factor-kappaB activation in macrophages. J Surg Res. 2004;116(2):253-61.

Sorrells SF, Caso JR, Munhoz CD, Sapolsky RM. The stressed CNS: when glucocorticoids aggravate inflammation. Neuron. 2009;64(1):33-9.

Sousa N, Almeida OF, Wotjak CT. A hitchhiker's guide to behavioral analysis in laboratory rodents. Genes Brain Behav. 2006;5 Suppl 2:5-24.

Sousa N, Almeida OF. Corticosteroids: sculptors of the hippocampal formation. Rev Neurosci. 2002;13(1):59-84.

Sousa N, Lukoyanov NV, Madeira MD, Almeida OF, Paula-Barbosa MM. Reorganization of the morphology of hippocampal neurites and synapses after stress-induced damage correlates with behavioral improvement. Neuroscience. 2000;97(2):253-66.

Sousa N, Madeira MD, Paula-Barbosa MM. Corticosterone replacement restores normal morphological features to the hippocampal dendrites, axons and synapses of adrenalectomized rats. J Neurocytol. 1999;28(7):541-58.

Sperlagh B, Illes P. Purinergic modulation of microglial cell activation. Purinergic Signal. 2007;3(1-2):117-27.

Stiles GL. Adenosine receptors. J Biol Chem. 1992;267(10):6451-4.

Sugama S, Takenouchi T, Fujita M, Kitani H, Conti B, Hashimoto M. Corticosteroids limit microglial activation occurring during acute stress. Neuroscience. 2013;232:13-20.

Svenningsson P, Hall H, Sedvall G, Fredholm BB. Distribution of adenosine receptors in the postmortem human brain: an extended autoradiographic study. Synapse. 1997;27(4):322-35.

Tanaka J, Fujita H, Matsuda S, Toku K, Sakanaka M, Maeda N. Glucocorticoid- and mineralocorticoid receptors in microglial cells: the two receptors mediate differential effects of corticosteroids. Glia. 1997;20(1):23-37.

Tremblay ME, Lecours C, Samson L, Sanchez-Zafra V, Sierra A. From the Cajal alumni Achucarro and Rio-Hortega to the rediscovery of never-resting microglia. Front Neuroanat. 2015;9:45.

Tremblay ME, Lowery RL, Majewska AK. Microglial interactions with synapses are modulated by visual experience. PLoS Biol. 2010;8(11):e1000527.

Tullin S, Hansen BS, Ankersen M, Moller J, Von Cappelen KA, Thim L. Adenosine is an agonist of the growth hormone secretagogue receptor. Endocrinology. 2000;141(9):3397-402.

Van de Velde S, Bracke P, Levecque K. Gender differences in depression in 23 European countries. Cross-national variation in the gender gap in depression. Soc Sci Med. 2010;71(2):305-13.

Vandevyver S, Dejager L, Tuckermann J, Libert C. New insights into the anti-inflammatory mechanisms of glucocorticoids: an emerging role for glucocorticoid-receptor-mediated transactivation. Endocrinology. 2013;154(3):993-1007.

Viau V, Meaney MJ. Variations in the hypothalamic-pituitary-adrenal response to stress during the estrous cycle in the rat. Endocrinology. 1991;129(5):2503-11.

Viau V, Soriano L, Dallman MF. Androgens alter corticotropin releasing hormone and arginine vasopressin mRNA within forebrain sites known to regulate activity in the hypothalamic-pituitary-adrenal axis. J Neuroendocrinol. 2001;13(5):442-52.

Vreeburg SA, Hoogendijk WJ, DeRijk RH, van Dyck R, Smit JH, Zitman FG, et al. Salivary cortisol levels and the 2-year course of depressive and anxiety disorders. Psychoneuroendocrinology. 2013;38(9):1494-502.

Waffarn F, Davis EP. Effects of antenatal corticosteroids on the hypothalamic-pituitary-adrenocortical axis of the fetus and newborn: experimental findings and clinical considerations. Am J Obstet Gynecol. 2012;207(6):446-54.

Wake H, Moorhouse AJ, Jinno S, Kohsaka S, Nabekura J. Resting microglia directly monitor the functional state of synapses in vivo and determine the fate of ischemic terminals. J Neurosci. 2009;29(13):3974-80.

Weaver DR. A_{2A} adenosine receptor gene expression in developing rat brain. Brain Res Mol Brain Res. 1993;20(4):313-27.

Westwood FR. The female rat reproductive cycle: a practical histological guide to staging. Toxicol Pathol. 2008;36(3):375-84.

Wittendorp MC, Boddeke HW, Biber K. Adenosine A3 receptor-induced CCL2 synthesis in cultured mouse astrocytes. Glia. 2004;46(4):410-8.

Yu L, Shen HY, Coelho JE, Araujo IM, Huang QY, Day YJ, et al. Adenosine A_{2A} receptor antagonists exert motor and neuroprotective effects by distinct cellular mechanisms. Ann Neurol. 2008;63(3):338-46.

Zimmermann H, Braun N, Kegel B, Heine P. New insights into molecular structure and function of ectonucleotidases in the nervous system. Neurochem Int. 1998;32(5-6):421-5.